

Oxo-Imido Molybdenum Trispyrazolyl Borate Complexes

By

Alev GÜNYAR

**A Dissertation Submitted to the
Graduate School in Partial Fulfillment of the
Requirements for the Degree of**

MASTER OF SCIENCE

**Department: Chemistry
Major: Chemistry**

**Izmir Institute of Technology
Izmir, Turkey**

July, 2004

We approve the thesis of **Alev GÜNYAR**

Date of Signature

.....

29.07.2004

Assoc. Prof. Dr. Isil TOPALOGLU SÖZÜER

Supervisor

Department of Chemistry

.....

29.07.2004

Prof. Dr. Fadime UGUR

Ege University,

Faculty of Science, Department of Chemistry

.....

29.07.2004

Prof. Dr. Levent ARTOK

Department of Chemistry

.....

29.07.2004

Prof. Dr. Levent ARTOK

Head of Department

ACKNOWLEDGEMENT

I wish to sincere thanks to my advisor Assoc. Prof. Isil Topaloglu Sözüer for her support and guidance in the completion of my research program.I would also thank my committee members Prof. Dr. Fadime Ugur and Prof. Dr. Levent Artok, for their help in editing and refining this manuscript.

I am thankful to Prof. Dr. Jon A. McCleverty for providing the Tp*(hydrotris(3,5-dimethylpyrazol-1-yl)borate) ligand.

I would thank to Dr. Ozan Sanli Sentürk for FAB-Mass spectra.

I want to thank to Dr. John C. Jeffery and H.Hamidov for solving the crystal structures.

Financial supports by the Research Foundation of Izmir Institue of Technology and TUBITAK are highly appreciated.

Many thanks to my friends and Dr. Hüseyin Özgener for their help and useful discussions.

Finally, I want to thank to my family for their love, pattience, understanding and support during my study and all my life.

ABSTRACT

Reaction of the oxo-molybdenum(V) compound, $[\text{MoTp}^*(\text{O})\text{Cl}_2]$, $[\text{Tp}^* = \text{hydrotris}(3,5\text{-dimethylpyrazol-1-yl})\text{borate}]$ with p-functionalized anilines $[\text{NH}_2\text{C}_6\text{H}_4\text{R}]$ (R = OMe, OEt, OPr, NO_2) in the presence of Et_3N under nitrogen, in toluene solution, afforded the novel oxo bridged oxo(arylimido) molybdenum(V) compounds $[\text{MoTp}^*(\text{O})\text{Cl}](\mu\text{-O})[\text{MoTp}^*(\text{Cl})(\equiv\text{NC}_6\text{H}_4\text{R})]$ (R = OMe, OEt, OPr, NO_2). Under same conditions, the reaction with aniline produced oxo bridged oxomolybdenum (V) compound, $[\text{MoTp}^*\text{OCl}]_2(\mu\text{-O})$.

The new compounds were characterized by FT-IR, FAB-Mass, and $^1\text{H-NMR}$ spectra. The single crystal X-ray crystallographic determination of $[\text{MoTp}^*(\text{O})\text{Cl}](\mu\text{-O})[\text{MoTp}^*(\text{Cl})(\equiv\text{NC}_6\text{H}_4\text{OMe})]$ was carried out to confirm that there is a Mo-O-Mo bridge and a near linear arylimido group in the structure.

ÖZ

Okso-molibden (V) , $[\text{MoTp}^*(\text{O})\text{Cl}_2]$, $[\text{Tp}^* = \text{hidrotris}(3,5\text{-dimetilpirazol})\text{borat}]$ kompleksinin p-fonksiyonel $[\text{NH}_2\text{C}_6\text{H}_4\text{R}]$ ($\text{R} = \text{OMe}, \text{OEt}, \text{OPr}, \text{NO}_2$) anilinlerle toluen çözeltilisinde, Et_3N varliginda, azot altinda reaksiyonlari sonucunda okso-köprülü okso(arilimido) molibden (V) bileşikleri olusmustur. Okso-molibden (V) kompleksinin ayni kosullarda anilinle reaksiyonu sonucunda ise okso köprülü okso molibden (V) $[\text{MoTp}^*\text{OCl}]_2(\mu\text{-O})$ bileşigi elde edilmiştir.

Yeni bileşiklerin yapıları, FT-IR, FAB-Mass, ve $^1\text{H-NMR}$ spektrumlarıyla aydinlatılmıştır. $[\text{MoTp}^*(\text{O})\text{Cl}](\mu\text{-O})[\text{MoTp}^*(\text{Cl})(\equiv\text{NC}_6\text{H}_4\text{OMe})]$ tek kristalinin yapisi X-isini kirinimi yöntemiyle çözülmüştür ve yapida Mo-O-Mo köprülü arilimido grubunun varligi ortaya çıkarılmıştır.

TABLE OF CONTENTS

LIST OF FIGURES	viii
LIST OF TABLES	x
LIST OF SCHEMES	xi
ABBREVIATIONS	xii
Chapter 1 INTRODUCTION	1
1.1. Molybdenum Trispyrazolyl Borate Chemistry.....	1
1.1.1. The Polypyrazolylborates	2
1.1.2. The Analogy Between Trispyrazolylborate and Cyclopentadienyl Ligand	3
1.2. Oxomolybdenum(V) Complexes Containig $\{\text{MoO}\}^{3+}$	5
1.2.1. Monomeric Oxo-Molybdenum(V) Complexes	6
1.2.2. Dimeric Species of Oxo-Molybdenum Complexes	8
1.2.3. Mixed-Valance Molybdenum (μ -O) Compounds	13
Chapter 2 EXPERIMENTAL STUDY.....	14
2.1. Experimental Techniques for Handling Air-Sensitive Compounds	14
2.2. Manipulation of Air-Sensitive Compounds	14
2.3. The Vacuum-Line Technique	14
2.3.1. The Double Manifold	14
2.3.2. The Schlenk Technique	17
2.4. Purification of Solvents	19
2.5. Experimental	20
2.6. Synthesis	21
2.6.1. $[\text{MoTp}^*(\text{O})\text{Cl}](\mu\text{-O})[\text{MoTp}^*(\text{Cl})(\equiv\text{NC}_6\text{H}_4\text{OMe})]$ (1)	21
2.6.2. $[\text{MoTp}^*(\text{O})\text{Cl}](\mu\text{-O})[\text{MoTp}^*(\text{Cl})(\equiv\text{NC}_6\text{H}_4\text{OEt})]$ (2).....	21
2.6.3. $[\text{MoTp}^*(\text{O})\text{Cl}](\mu\text{-O})[\text{MoTp}^*(\text{Cl})(\equiv\text{NC}_6\text{H}_4\text{OPr})]$ (3).....	21

2.6.4. [MoTp*(O)Cl](μ -O)[MoTp*(Cl)(\equiv NC ₆ H ₄ NO ₂)] (4)	22
2.6.5. [MoTp*(O)Cl](μ -O)[MoTp*(O)(Cl)] (5)	22
Chapter 3 RESULT AND DISCUSSION	23
3.1. Synthetic Studies	23
3.2. Crystallographic Studies	27
3.2.1. Crystal Structure Determination and Refinement	27
3.2.2. Crystal Structure of [MoTp*(O)Cl](μ -O)[MoTp*(Cl)(\equiv NC ₆ H ₄ OMe)]	29
3.3. Spectroscopic studies	34
CHAPTER 4 CONCLUSION	49
REFERENCES	50

LIST OF FIGURES

Figure 1.1. Pyrazole nucleous (1), and pyrazolide ion (2).....	1
Figure 1.2. Preperation of Polypyrazolylborates	2
Figure 1.3. Comparison of Trispyrazolborate and Cyclopentadienyl Ligand Coordination.....	3
Figure 1.4. Hydrotris 1-pyrazolyl borate ion (Tp : R = H, Tp* : R = Me)	4
Figure 1.5. Comparison of Tp and Tp*, showing cone angles	5
Figure 1.6. The structures of [MoTp*(O)C ₂] (3) and [MoTp(O)C ₂] (4)	7
Figure 1.7. The Crystal Structure of [MoTp(O)C ₂] (4)	7
Figure 1.8. Crystal structure of [MoTpOCl] ₂ O (cis isomer)	9
Figure 1.9. Crystal structure of (MoTpOCl) ₂ O (trans isomer)	10
Figure 1.10. Solvent dependence of the reactions of [MoTp*(O)C ₂]	11
Figure 1.11. Crystal structure of [MoTp*O(Cl)] ₂ (μ-O)	12
Figure 1.12. The Structures of Complexes (5), (6), (7), (8)	13
Figure 1.13. Crystal structure of [Mo ^V Tp*(O)Cl](μ-O)[Mo ^{VI} Tp*(O) ₂].....	14
Figure 2.1. The Double Manifold	16
Figure 2.2. Cross section through a double oblique tap	16
Figure 2.3. Bubbler	17
Figure 2.4. The Complete Set-up.....	17
Figure 2.5. Schlenk Tube	18
Figure 2.6. Transferring a liquid sample	19
Figure 2.7. Filtering a liquid sample.....	19
Figure 2.8. Solvent Stil	20
Figure 3.1. The Structures of p-Functionalized Anilines	25
Figure 3.2. The structures for the complexes (1), (2), (3), (4).....	26
Figure 3.3. The structure for the complex (5).....	26
Figure 3.4. Crystal Structure of [MoTp*(O)Cl](μ-O)[MoTp*(Cl)(≡NC ₆ H ₄ OMe)].....	29
Figure 3.5. Linear (a) and bent (b) imido linkages	32
Figure 3.6. FT-IR spectrum of [MoTp*(O)Cl](μ-O) [MoTp*Cl(^o NC ₆ H ₄ OMe)](1)	37
Figure 3.7. ¹ H-NMR spectrum of [MoTp*(O)Cl](μ-O) [MoTp*Cl(^o NC ₆ H ₄ OMe)] (1)	37
Figure 3.8. FT-IR spectrum of [MoTp*(O)Cl](μ-O) [MoTp*Cl(^o NC ₆ H ₄ OEt)](2)	39

Figure 3.9. $^1\text{H-NMR}$ spectrum of $[\text{MoTp}^*(\text{O})\text{Cl}](\mu\text{-O}) [\text{MoTp}^*\text{Cl}(\text{}^\circ\text{NC}_6\text{H}_4\text{OEt})]$ (2) ...	39
Figure 3.10. FT-IR spectrum of $[\text{MoTp}^*(\text{O})\text{Cl}](\mu\text{-O}) [\text{MoTp}^*\text{Cl}(\text{}^\circ\text{NC}_6\text{H}_4\text{OPr})]$ (3)	41
Figure 3.11. $^1\text{H-NMR}$ spectrum of $[\text{MoTp}^*(\text{O})\text{Cl}](\mu\text{-O}) [\text{MoTp}^*\text{Cl}(\text{}^\circ\text{NC}_6\text{H}_4\text{OPr})]$ (3).	41
Figure 3.12. FT-IR spectrum of $[\text{MoTp}^*(\text{O})\text{Cl}](\mu\text{-O}) [\text{MoTp}^*\text{Cl}(\text{}^\circ\text{NC}_6\text{H}_4\text{NO}_2)]$ (4)	43
Figure 3.13. $^1\text{H-NMR}$ spectrum of $[\text{MoTp}^*(\text{O})\text{Cl}](\mu\text{-O}) [\text{MoTp}^*\text{Cl}(\text{}^\circ\text{NC}_6\text{H}_4\text{NO}_2)]$ (4).	43
Figure 3.14. FT-IR spectrum of $[\text{MoTp}^*(\text{O})\text{Cl}](\mu\text{-O}) [\text{MoTp}^*\text{Cl}(\text{O})]$ (5)	45
Figure 3.15. $^1\text{H-NMR}$ spectrum of $[\text{MoTp}^*(\text{O})\text{Cl}](\mu\text{-O}) [\text{MoTp}^*\text{Cl}(\text{O})]$ (5).....	45
Figure 3.16.FAB-Mass spectrum of $[\text{MoTp}^*(\text{O})\text{Cl}](\mu\text{-O}) [\text{MoTp}^*\text{Cl}(\text{}^\circ\text{NC}_6\text{H}_4\text{OMe})]$ (1)	47
Figure 3.17 FAB-Mass spectrum of $[\text{MoTp}^*(\text{O})\text{Cl}](\mu\text{-O})[\text{MoTp}^*\text{Cl}(\text{}^\circ\text{NC}_6\text{H}_4\text{ONO}_2)]$ (4)	48

LIST OF TABLES

Table 3.1. Crystal data and structure refinement for [MoTp*(O)Cl](μ -O) [MoTp*Cl($^{\circ}$ NC ₆ H ₄ OMe)].....	28
Table 3.2. Selected bond lengths (\AA) and angles ($^{\circ}$) for [MoTp*(O)Cl](μ -O) [MoTp*(Cl)(\equiv NC ₆ H ₄ OMe)]	30
Table 3.3. Atomic coordinates ($\times 10^4$) and equivalent isotropic displacement parameters ($\text{\AA}^2 \times 10^3$) for K1m. U(eq) is defined as one third of the trace of the orthogonalized U _{ij} tensor	33
Table 3.4. FT-IR Data for the New Complexes.....	35
Table 3.5. ¹ H-NMR data of [MoTp*(O)Cl](μ -O) [MoTp*Cl($^{\circ}$ NC ₆ H ₄ OMe)](1)	38
Table 3.6. ¹ H-NMR data of [MoTp*(O)Cl](μ -O) [MoTp*Cl($^{\circ}$ NC ₆ H ₄ OEt)](2).....	40
Table 3.7. ¹ H-NMR data of [MoTp*(O)Cl](μ -O) [MoTp*Cl($^{\circ}$ NC ₆ H ₄ OPr)](3)	42
Table 3.8. ¹ H-NMR data of [MoTp*(O)Cl](μ -O) [MoTp*Cl($^{\circ}$ NC ₆ H ₄ NO ₂)](4).....	44
Table 3.9. ¹ H-NMR data of [MoTp*(O)Cl](μ -O) [MoTp*Cl(O)](5)	46
Table 3.10. FAB-Mass data of the new complexes (1)and (4).....	46

LIST OF SCHEMES

Scheme 1.1. Formation of μ -oxo species	9
Scheme 3.1. Synthetic route for the new compounds (1)-(4) (R = OMe, OEt, OPr, NO ₂) .	25

ABBREVIATIONS

Tp : Trispyrazolylborate

Tp* : Tris (3,5-dimethylpyrazolyl)borate

Cp : Cyclopentadienyl

Cp* : Pentamethyl cyclopentadienyl

Tp^{Pr} : Hydrotris (3-isopropylpyrazolyl)borate

KTp* : Potassium hydrotris (3,5-dimethylpyrazolyl)borate

Et₃N : Triethylamine

Me : Methyl

Et : Ethyl

Pr : Propyl

FT-IR : Fourier Transform Infrared

NMR : Nuclear Magnetic Resonance

δ : Chemical Shift

FAB : Fast Atom Bombardment

M⁺ : Molecular ion

Mol. wt. : Molecular weight

TLC : Thin Layer Chromatography

CHAPTER 1

INTRODUCTION

1.1 Molybdenum Trispyrazolyl Borate Chemistry

1.1.1 The Polypyrazolylborates

The pyrazole nucleus, 1, is thermally and hydrolytically very stable. As a ligand, it coordinates to metals and metalloids through the 2-N, as do 1-alkylpyrazoles. When deprotonated, pyrazole becomes the pyrazolide ion, 2, which can coordinate through both nitrogen atoms as an exobidentate [1] ligand of C_{2v} symmetry. The nucleophilicity of the nitrogens and their steric accessibility may be varied through appropriate ring substitution [2].

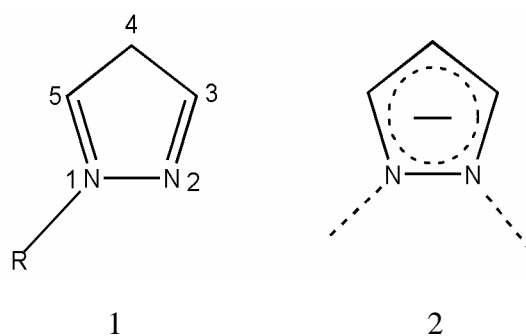


Figure 1.1. Pyrazole nucleus (1), and pyrazolide ion (2)

The polypyrazolylborate ligands $[BR_n(Pz)_{4-n}]^-$ were first synthesized by Trofimenko in 1966 [3] and the coordination chemistry of these ligands has been a vigorous research area [4]. It has been shown that there are strong analogies between the behaviour of metal complexes containing trispyrazolylborato anions, and those containing η^5 -cyclopentadienyl ligand [5]. This ligand system has widely been used in inorganic and organometallic chemistry especially with d and f transition elements [6]. It was known that tris(pyrazolyl)borate ligands have had a significant impact on the

modelling of active centre of Mo enzymes [7]. Also these ligands exhibit dynamic behaviour on the NMR time scale [8]. The sterically encumbering nature of the Tp* (hydrotris(3,5-dimethylpyrazolyl)borate) ligand compared with Cp* (pentamethyl cyclopentadienyl) is widely known and explored in high activity for catalyst systems [9,10]. Their synthesis is easily accomplished by the reaction of pyrazole or a substituted pyrazole with an alkali borohydride salt, the extent of substitution being controlled by adjusting the temperature [11]. (Figure 1.2)

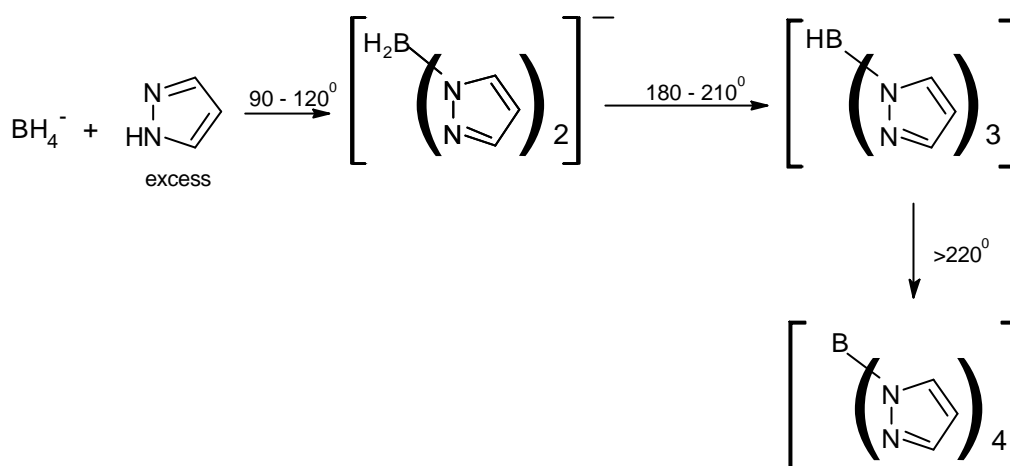


Figure 1.2. Preparation of Polypyrazolylborates

In all these uni-negative species, the boron exist in a tetrahedral environment and coordination to a metal ion occurs via the nitrogen atoms in the 2-position in each pyrazolyl ring. Bispyrazolylborates are therefore bidentate, while trispyrazolylborates are tridentate and occupy three facial coordination sites in its metal complexes. The facial coordination to three sites of metal ion, their uni-negative charge donation of six electrons to the metal has resulted in a comparison with the cyclopentadienyl anion as a ligand [2].

1.1.2 The Analogy Between Trispyrazolylborate and Cyclopentadienyl Ligands

Throughout the years, polypyrazolylborates have been compared to cyclopentadienyl ligand. They are monoanionic, formally six electron donors which can occupy three facial coordination sites on a metal ion [12].

One of the several advantages of the tris(1-pyrazolyl)borate ion, Tp^- , over the cyclopentadienide ion as a ligand is that by appropriate substitution on the pyrazole ring some can alter the steric and/or electronic environment of the metal ion without destruction of the symmetry of the parent ligand. It had been found before that the presence of alkyl substituents in the 3 positions as in $\text{MoTp}^*(\text{CO})_3$ increases the electron density on Mo, at the same time restricting the access to the metal by prospective reactants. The result is increased stability of derivatives, coupled with greater difficulty in effecting reactions that proceed through a sterically hindered transition state [13].

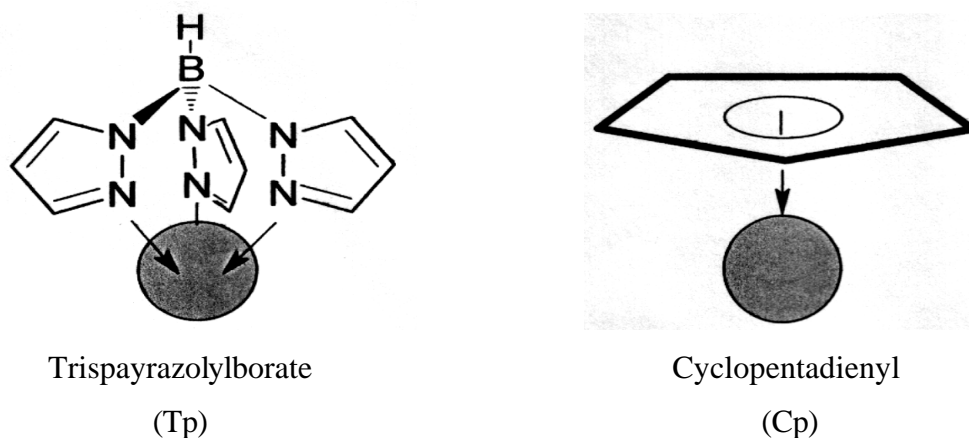


Figure 1.3. Comparison of Trispyrazolborate and Cyclopentadienyl Ligand Coordination

Trispyrazolylborates are tripodal with C_{3v} symmetry, unlike the D_{5h} pentagonal cyclopentadienyl ligand, and the trispyrazolylborates also have a much greater steric bulk [11]. The electronic binding properties of the two ligands are also different. Cyclopentadienyl ligands bind to metal by carbon-to-metal p -donation from ring p -

molecular orbitals and also p-acceptance into ring orbitals. The trispyrazolylborates function as a nitrogen-to-metal s-donor and a weak p-acceptor [14]. Trispyrazolylborates are better donors and comparable acceptors than cyclopentadienyl.

Molybdenum-trispyrazolylborates are mainly six coordinate in contrast to the predominately seven coordinate species found in the analogous molybdenum-cyclopentadienyl chemistry. This is partially due to the steric effects of trispyrazolylborates, but also to the electronic influences of these ligands. The highly directional s-orbitals on the nitrogens help hybridise the metal into an octahedrally coordinate structure. The highly diffuse p-orbitals of cyclopentadienyl have no such influence on the metal [15].

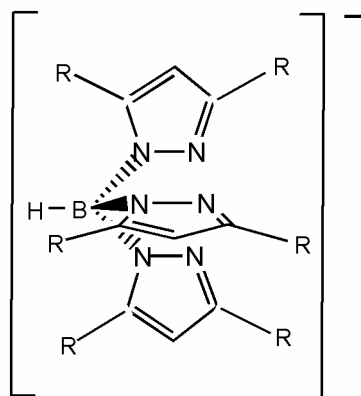


Figure 1.4. Hydrotris 1-pyrazolyl borate ion (Tp : R = H, Tp* : R = Me)

There is evidence to show that the trispyrazolylborate ligand forms stronger bonds to metals than cyclopentadienyl. Combined with the extra steric protection afforded this means that metal complexes of the trispyrazolylborato anions are generally more thermodynamically stable. Thus stable trispyrazolylborato complexes have become more abundant than their cyclopentadienyl predecessors [15, 16].

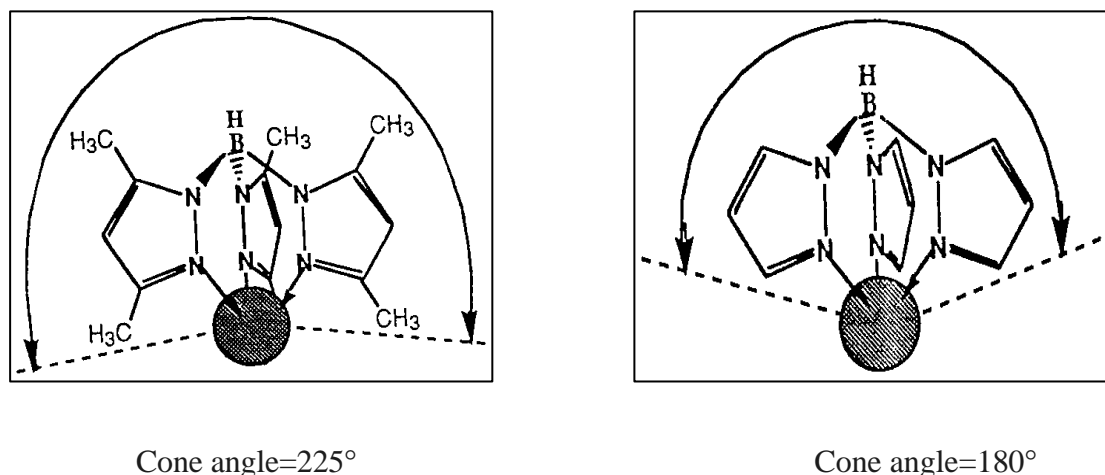


Figure 1.5. Comparison of Tp and Tp*, showing cone angles.

This is an extremely bulky ligand and the methyl groups in the 3-position help to envelop the metal in its coordination compounds. This can be seen from the Tolman cone angles for trispyrazolylborate, tris-(3,5-dimethylpyrazolyl)borate, cyclopentadienyl and pentamethylcyclopentadienyl ligands which are 180°, 225°, 136°, 165° respectively [17].

It is the steric and electronic properties of this tris-(3,5-dimethylpyrazolyl)borate ligand that brings about stabilisation of formally coordinatively unsaturated complexes or, in many cases compounds which are otherwise air and moisture sensitive [17].

1.2 Oxomolybdenum(V) Complexes Containig {MoO}³⁺

Molybdenum which is considered as a trace element, presents several oxidation states, and therefore may change easily its coordination number and to form mono and binuclear oxo complexes which is of great importance from basic as well as applied points of view. The propensity of oxo-molybdenum species in higher oxidation states to form di,tri,and polynuclear complexes is well known [18]. Molybdenum is a relevant element for the synthesis of many homogeneous and heterogeneous catalyst. The element is also essential in several enzymatic systems. One of the characteristics of the molybdenum chemistry is related to the easy conversation between its oxidation states and to the changes of coordination number, observed particularly between Mo(III), Mo(IV), Mo(V), and Mo(VI). The chemistry of oxo Mo(V) complexes is of importance especially in industrial and biochemical catalysis [19].

Oxo and imido ligands form commonly multiple bonds when attached to transition metal centres. The chemistry of the corresponding complexes has experienced a remarkable growth during past 15 years. Both the oxo and imido groups permit stabilization of high formal oxidation states [20].

Recently, interest in chemistry of transition metal compounds that contain multiple bonded ligands has increased greatly due mainly to their involvement in many important reactions. Although quite a large number of bis(imido) [21-25] and dioxo [26] complexes of molybdenum are known, there is only small information on the related mixed terminal oxo-imido compounds [27-31]. Although a number of systems involving μ -ligation in the presence of terminal imido groups have previously been reported [24-31], only a few examples of molybdenum compounds containing both imido ligands and tris(pyrazolyl)borate co-ligand were known [22, 25, 32]. However, the area of μ -oxo complexes containing mixed oxo-arylimido ligands and Tp* co-ligand is still largely unexplored.

1.2.1 Monomeric Oxo-Molybdenum(V) Complexes

[MoTp*(O)Cl₂] was first reported by Trofimenko by alumina treatment of the uncharacterized red solution that he obtained from the reaction of [MoTp*(CO)₃] with SOCl₂ [13]. The red solution has since been characterized as containing MoTp*(Cl)₃ [33], and it was found that the oxidation of this compound with dioxygen gave a good yield of the yellow-green crystalline complex [MoTp*(O)Cl]₂. [MoTp(O)Cl]₂ was made in analogous manner. These monomers are paramagnetic, as expected for a d¹ system.[34]

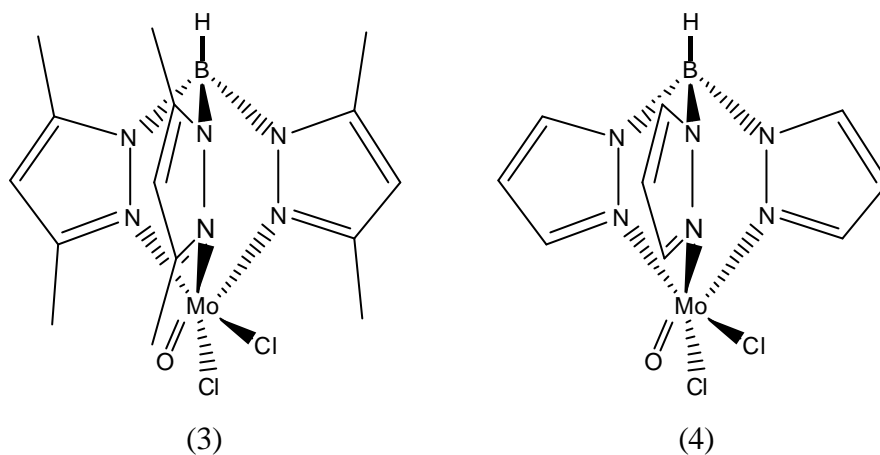


Figure 1.6. The structures of $[\text{MoTp}^*(\text{O})\text{Cl}_2]$ (3) and $[\text{MoTp}(\text{O})\text{Cl}_2]$ (4)

The X-ray crystal structure of $[\text{MoTp}(\text{O})\text{Cl}_2]$ (4) is given in figure 1.7

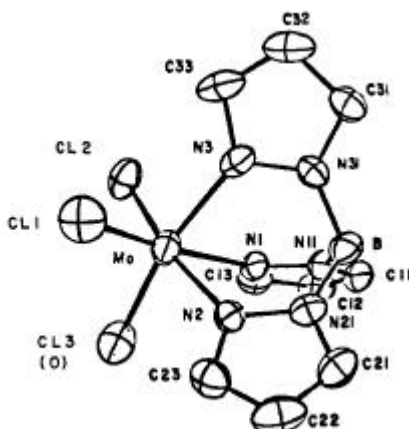
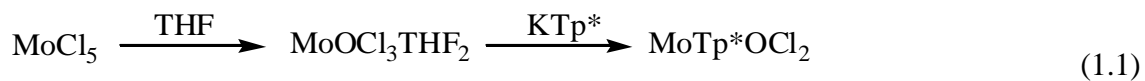


Figure 1.7 The Crystal Structure of $[\text{MoTp}(\text{O})\text{Cl}_2]$ (4)

However, Enemark's group have developed a more convenient preparation for $[\text{MoTp}^*\text{OCl}_2]$. Reaction of MoCl_5 with tetrahydrofuran (THF) under anaerobic conditions (1.1) yields the known $\text{MoOCl}_3(\text{THF})_2$,



Presumably by abstraction of an oxygen atom from the solvent addition of KTp^* to the reaction mixture and moderate heating affords $[\text{MoTp}^*\text{OC}_2]$ as a green precipitate, which can be recrystallised from hot dichloromethane or 1,2-dichloroethane as bright green crystals. Typical yields are 50-70 %. The complex is stable in air indefinitely, is stable to water, and is unchanged at 200 °C [35].

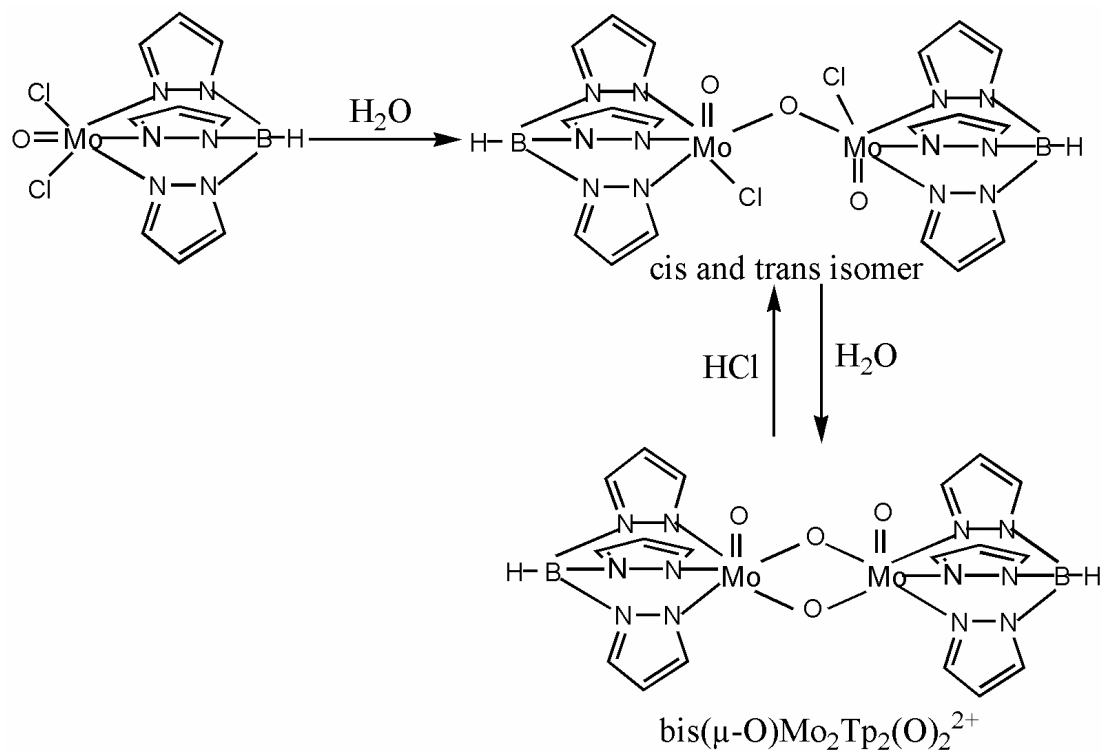
There is no evidence for ligand substitution reactions of $[\text{MoTp}^*\text{OC}_2]$ at room temperature. Ligand-exchange reactions of $[\text{MoTp}^*\text{OC}_2]$ probably proceed by dissociation of chloride and subsequent coordination of the new ligand [35].

$[\text{MoTp}^*\text{OCl}]^+$ fragment is very attractive to work with, because: (i) it is electronically simple (d^1), (ii) it is both redox active and paramagnetic, (iii) it is synthetically easy to use, and (iv) the coordination chemistry and bioinorganic chemistry of oxo-molybdenum (V) complexes in general have been extensively studied, so their spectroscopic properties are fairly thoroughly understood [36].

Enemark and his coworkers have prepared a variety of derivatives from $\text{MoTp}^*(\text{O})\text{C}_2$, $[\text{MoTp}^*(\text{O})\text{Cl}(\text{OR})]$, $[\text{MoTp}^*(\text{O})\text{Cl}(\text{SR})]$, $[\text{MoTp}^*(\text{O})\{\text{E}(\text{CH}_2)_n\text{E}\}]$ ($\text{E} = \text{O}$ or S) and $[\text{MoTp}^*(\text{O})(\text{cat})]$ (cat represents the dianion of a range of catechols, 1,2-dihydroxybenzenes) [37, 38, 39]

1.2.2 Dimeric Species of Oxo-Molybdenum Complexes

$[\text{MoTp}(\text{O})\text{C}_2]$ was prepared by the reaction O_2 with $[\text{MoTp}(\text{Cl})_3]$. A pair of $[\text{TpMo}(\text{O})\text{C}_2]\text{O}$ geometric isomers (cis and trans) and $[\text{TpMo}_2(\text{O})_2](\mu\text{-O})_2$ were obtained from the reaction of MoC_5 and KTp in dilute HCl . Hydrolysis of the $\text{Mo}(\text{V})$ complex $[\text{MoTp}(\text{O})\text{C}_2]$ leads to two geometric isomers of the formula $[(\text{MoTp}(\text{O})\text{Cl})_2]\text{O}$ (Scheme 1.1). Crystal structure of the geometric isomers show them to be linear $\mu\text{-O}$ bridged Mo-O-Mo . Further hydrolysis of the geometric isomers indicates to a final bis $(\mu\text{-O})\text{Mo}_2\text{O}_4^{2+}$ species [34,40].



Scheme 1.1 Formation of μ -oxo species

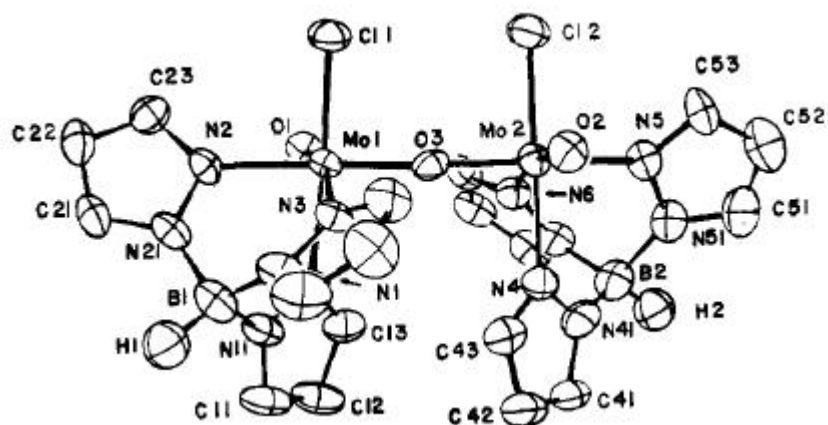


Figure 1.8. Crystal structure of $[\text{MoTpOCl}]_2\text{O}$ (cis isomer)

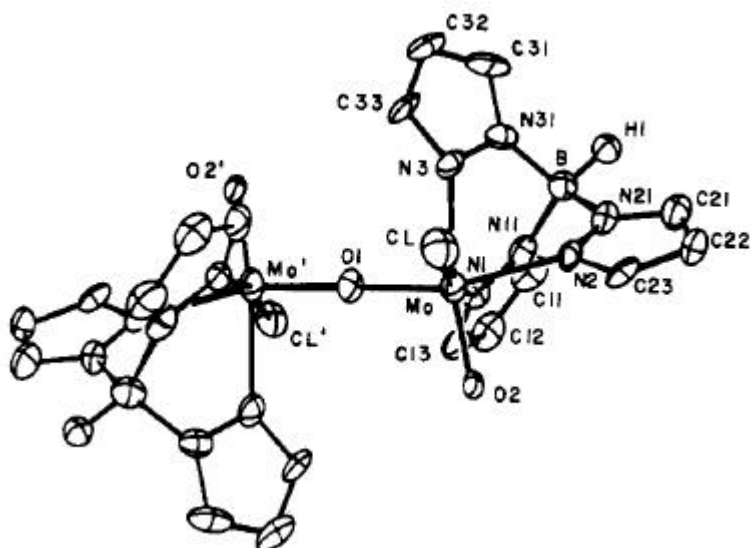


Figure 1.9. Crystal structure of $(\text{MoTpOCl})_2\text{O}$ (trans isomer)

The oxo-bridged Mo(V) compounds $[\text{MoTp}^*\text{OCl}]_2(\mu\text{-O})$ were previously reported by different methods by different research groups.

Enemark and co-workers prepared the compound $[\text{MoTp}^*\text{O}_2]_2(\mu\text{-O})$ by the treatment of $[\text{MoTp}^*(\text{O})_2\text{Br}]$ with aqueous ammonia solution in dry dichloromethane. A net equation for its formation is;



This reaction demonstrates that the Tp^* ligand alone is not bulky enough to prevent condensation of dioxo-Mo(VI) complexes and that the size and nature of the coligand X can have dramatic effects on a complex's ability to undergo condensation or dinucleation [41].

Enemark and co-workers synthesized the $[\text{MoTp}^*(\text{O})\text{Cl}]_2(\mu\text{-O})$ compound by the reaction of the $[\text{MoTp}^*(\text{O})_2\text{X}]$ complex with triphenylphosphine (Ph_3P) in toluene. As shown in figure 1.10., in all reactions, in the first step, regardless of solvent, oxygen atom transfer from the $[\text{MoO}_2]^{2+}$ moiety to Ph_3P was appeared. In chlorinated solvents, the oxygen atom transfer reaction was followed by abstraction of a chlorine atom from the solvent to yield $[\text{MoTp}^*(\text{O})\text{ClX}]$ as the final product. In toluene, despite the steric barrier provided by the 3-methyl groups of Tp^* , comproportionation of the

initial Mo(IV) product with the starting Mo(VI) complex occurs to yield a binuclear Mo(V) complex [42].

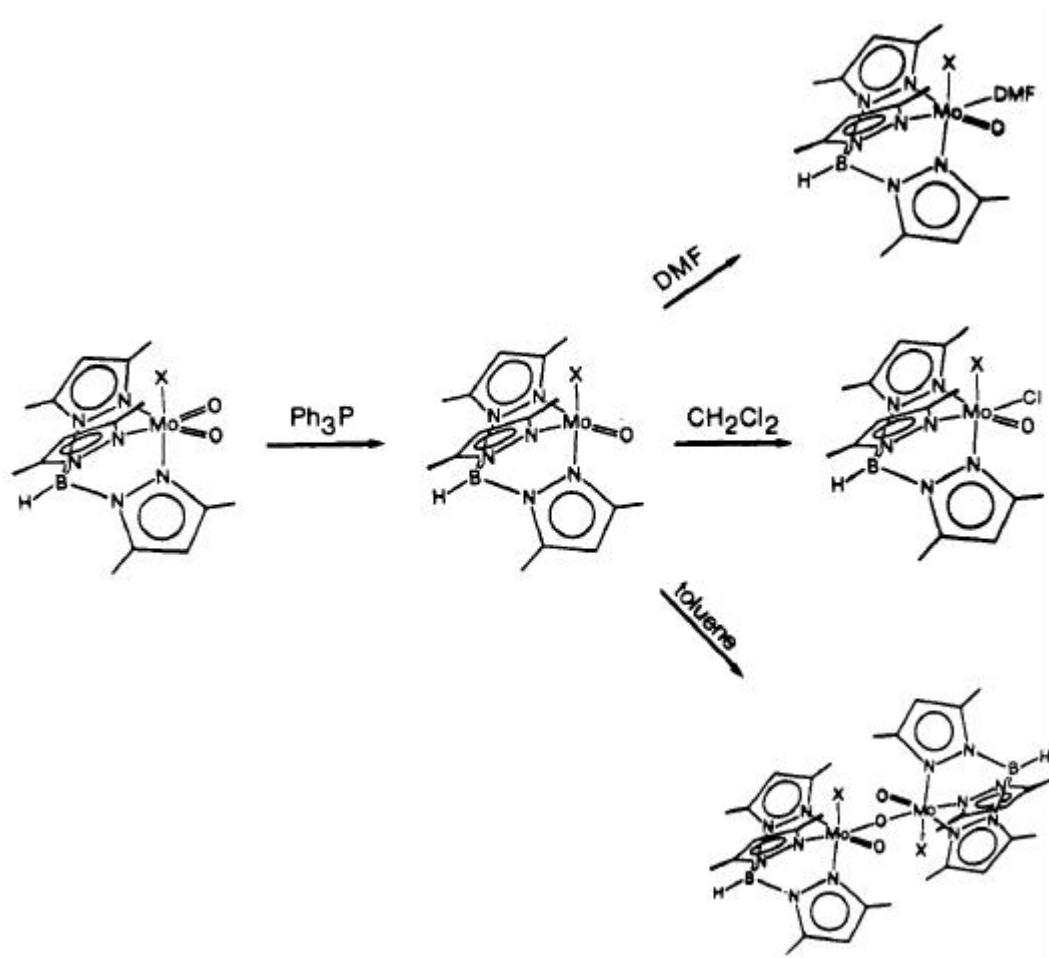


Figure 1.10. Solvent dependence of the reactions of $[\text{MoTp}^*(\text{O})_2\text{X}]$

Millar et. al. reported that the treatment of a mixture of 1,3-dimethoxy-para-tert-butylcalix(4)arene and $[\text{MoTp}^*\text{OC}_2\text{H}_5]$ in toluene in the presence of excess triethylamine resulted the compound, $[\text{MoTp}^*(\text{O})\text{Cl}]_2(\mu\text{-O})$ in the absence of calixarene due to the presence of adventitious water. The crystal structure of $[\text{MoTp}^*(\text{O})\text{Cl}]_2(\mu\text{-O})$ is shown in figure 1.11. [43].

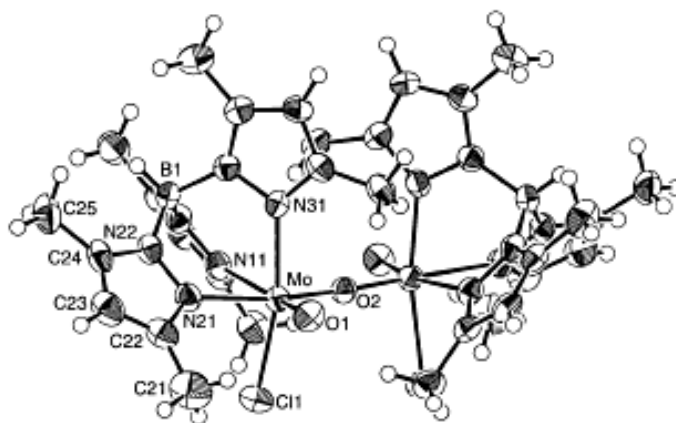


Figure 1.11. Crystal structure of $[\text{MoTp}^*\text{O}(\text{Cl})]_2(\mu\text{-O})$

McCleverty et. al. have prepared the compound $[(\text{MoTp}^*\text{OCl})_2](\mu\text{-O})$ by the reaction of $[\text{MoTp}^*\text{O}_2\text{Cl}]$ with Ph_3P in wet (i.e. not distilled) toluene containing approximately 0,03% water [44].

McCleverty et.al. reported that the reaction of $[\text{MoTp}^*\text{OCl}_2]$ with arylamines RNH_2 ($\text{R} = \text{C}_6\text{H}_4\text{Me}$, $\text{C}_6\text{H}_4\text{NMe}_2$, $\text{NH}_2\text{C}_6\text{H}_4$) in toluene in the presence of Et_3N resulted the mononuclear compounds $[\text{MoTp}^*(\text{O})\text{Cl}(=\text{NR})]$ [$\text{R} = \text{C}_6\text{H}_4\text{Me}$ (5), $\text{C}_6\text{H}_4\text{NMe}_2$ (6), $\text{C}_6\text{H}_4\text{NH}_2$ (7)] and dinuclear compound $[\text{MoTp}^*(\text{O})\text{Cl}]_2(\text{NC}_6\text{H}_4\text{N})$ (8) [27].

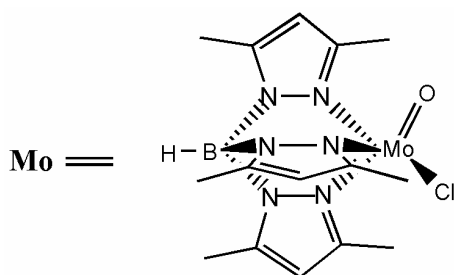
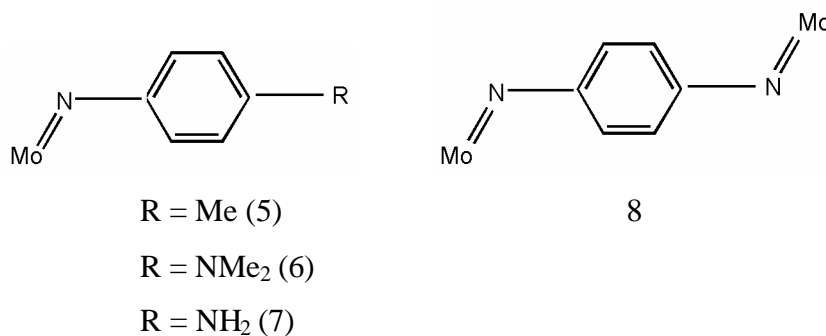


Figure 1.12. The Structures of Complexes (5), (6), (7), (8)

1.2.3. Mixed-Valance Molybdenum (μ -O) Compounds

Reaction of $[\text{Mo}^{\text{VI}}\text{Tp}^*\text{O}_2\text{Cl}]$ with the grignard reagent RMgX (R: Me, PhCH₂ ; X:Cl, I, Br) produce coordinatively unsaturated $[\text{Mo}^{\text{V}}\text{Tp}^*\text{O}_2]$ compound. Reaction of $[\text{Mo}^{\text{V}}\text{Tp}^*(\text{O})_2]$ with $[\text{Mo}^{\text{VI}}\text{Tp}^*(\text{O})_2\text{Cl}]$ to form $[\text{Mo}^{\text{V}}\text{Tp}^*(\text{O})\text{Cl}](\mu\text{-O})[\text{Mo}^{\text{VI}}\text{Tp}^*(\text{O})_2]$. Its crystal structure is shown in figure 1.14 [45].

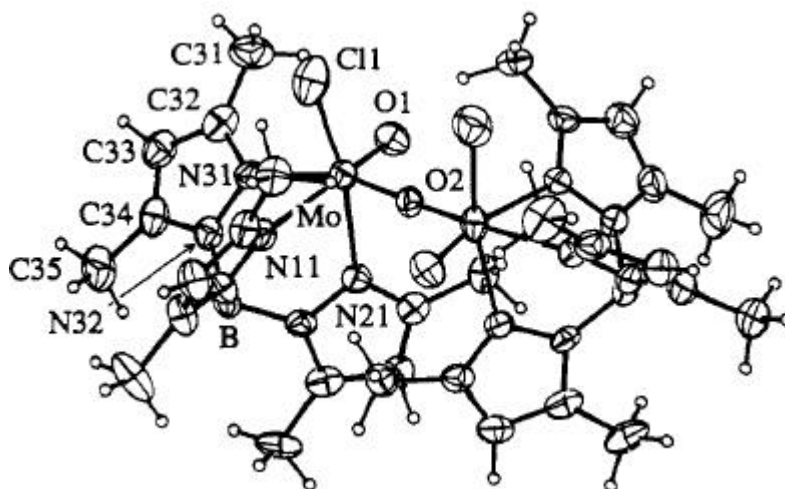


Figure 1.14. Crystal structure of $[\text{Mo}^{\text{V}}\text{Tp}^*(\text{O})\text{Cl}](\mu\text{-O})[\text{Mo}^{\text{VI}}\text{Tp}^*(\text{O})_2]$

CHAPTER 2

EXPERIMENTAL STUDY

2.1. Experimental Techniques for Handling Air-Sensitive Compounds

Many compounds are air sensitive and tend to decompose if not handled properly. Although handling air-sensitive compounds may at first appear cumbersome, under proper precautions and with appropriate manipulation tools and techniques, they may be handled almost as easily as ordinary compounds [46].

2.2. Manipulation of Air-Sensitive Compounds

For carrying out experiments with exclusion of air the following techniques are employed;

- a) Vacuum-Line Technique
- b) Schlenk Technique

Depending on the objectives and air sensitivity of the compounds handled, one technique or a combination of techniques are used. Techniques using the vacuum-line and schlenk glassware are sufficient and convenient for most purposes of handling air-sensitive compounds [46].

2.3. The Vacuum-Line Technique

2.3.1. The Double Manifold

Carrying out reactions under dry and/or inert conditions as a matter of routine, the double manifold is the most useful item of equipment that will enable you to do this. (Figure 2.1) [47].

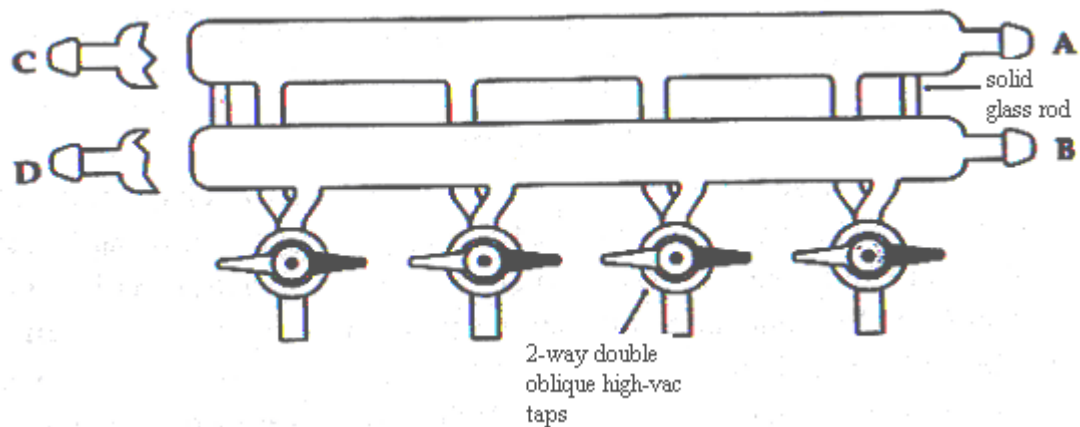


Figure 2.1. The Double Manifold

Connections:

A connected an inert gas cylinder via a bubbler (unless bubbler attached at C)

B connected to a vacuum pump via a trapping system

C (optional outlet) connected to bubbler

D (optional outlet) connected to vacuum gauge

The double manifold consists of two glass barrels, one evacuated and one filled with an inert gas. An outlet is supplied by either barrel of the manifold via a two-way double oblique tap (Figure 2.2.).

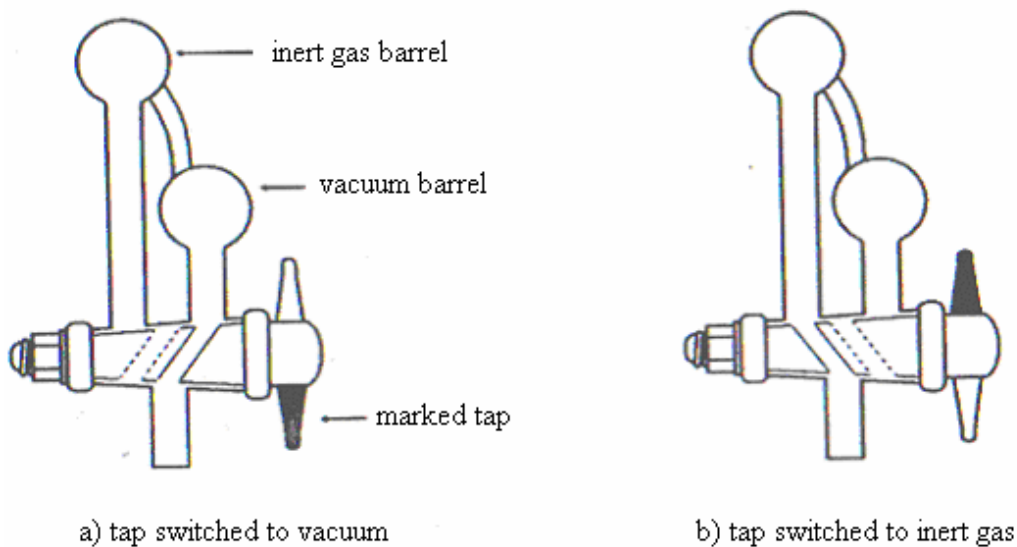


Figure 2.2. Cross section through a double oblique tap

A bubbler should be incorporated in the line from the cylinder which feeds the inert gas barrel and it should have a built in anti suck-back valve to avoid oil contaminating the manifold (Figure 2.3.).

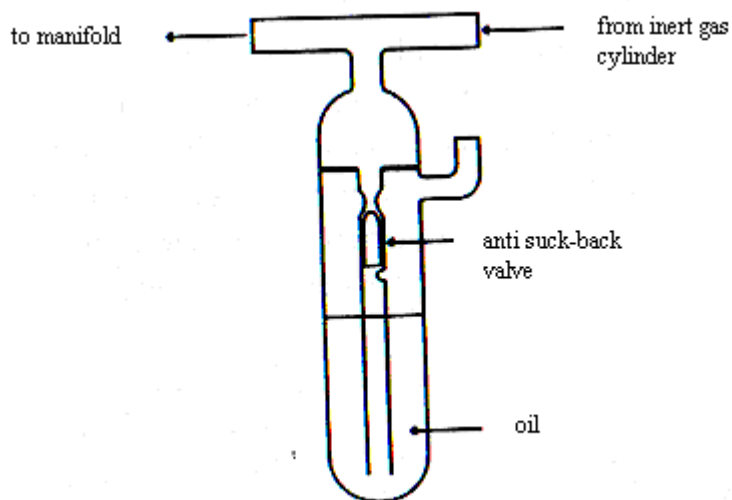


Figure 2.3. Bubbler

A rotary pump is normally connected to the vacuum barrel of the manifold and a schematic diagram showing the complete set up is shown in figure 2.4.

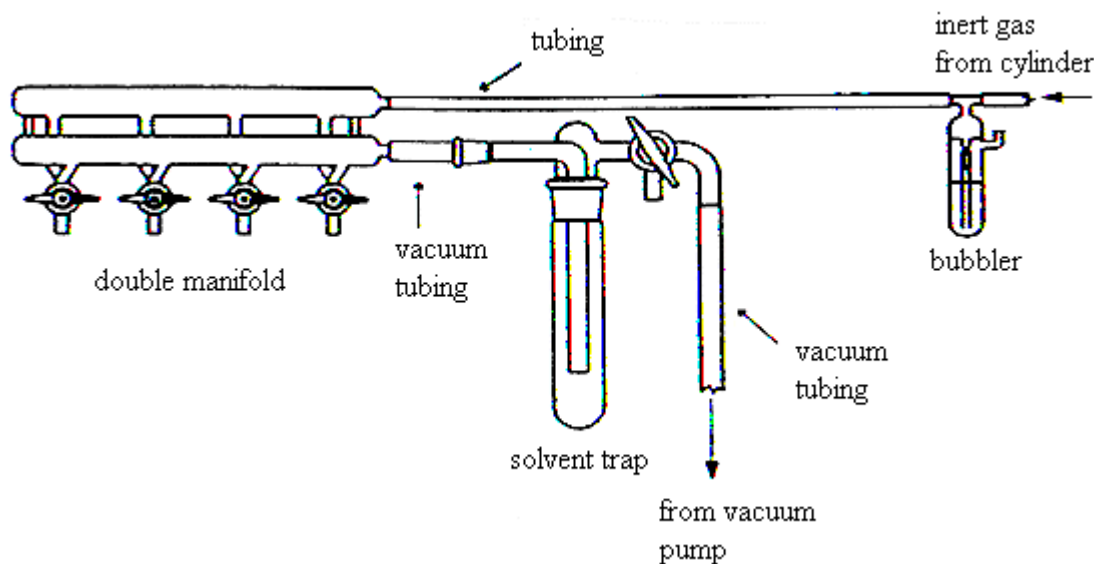


Figure 2.4. The Complete Set-up

2.3.2. The Schlenk Technique

The basic and simplest schlenk tube is shown in figure 2.5. With the schlenk tube one can transfer a solid or liquid in an atmosphere of an inert gas, such as nitrogen and argon [46,48].

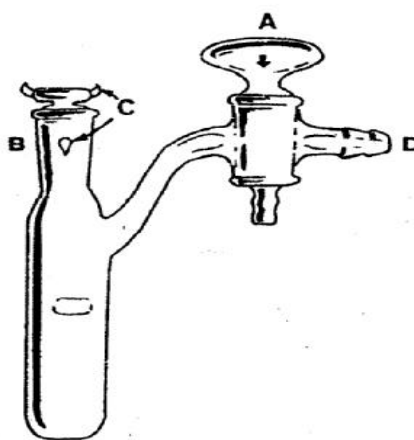


Figure 2.5. Schlenk Tube

The inlet is equipped with a stopcock (A) and the main opening has a standard taper (B), which has a small glass ears (C) to hold the stopper or other component with rubber bands or small metal springs. Manipulation of air-sensitive compounds are carried out as follows;

The schlenk tube is stoppered and evacuated by pumping through D. By introducing the inert gas through A, the tube is filled with the inert gas. The usual operation is to repeat the evacuation and the filling cycle a few times. Figure 2.5 shows the schlenk tube fitted with a two-way stopcock that can be used both for evacuation and for filling with inert gas. The tap is turned through 90° to let gas pass through the tail part and then is turned another 90° to allow gas into the flask.

Transfer of liquid can be performed by using a syringe with a long needle as shown in figure 2.6.

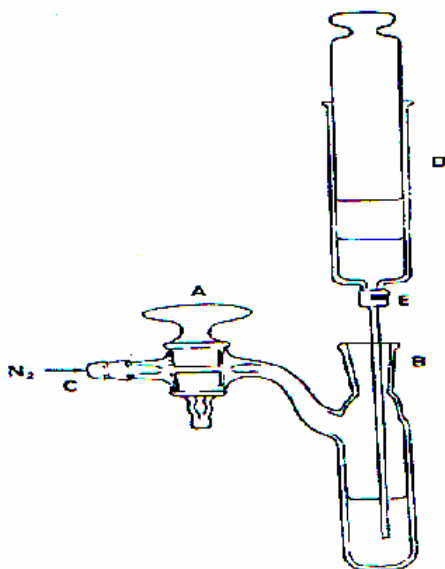


Figure 2.6. Transferring a liquid sample

Transfer of a liquid sample and filtration can be accomplished as shown in figure 2.7.

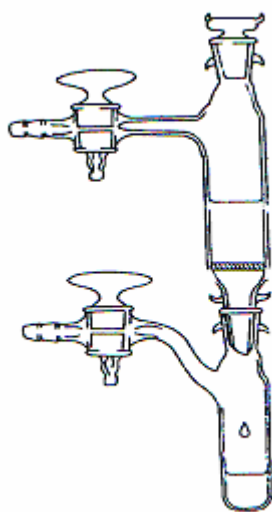


Figure 2.7. Filtering a liquid sample

2.4. Purification of Solvents

The solvents used are purified, dried under nitrogen by distillation system. A solvent still is used for this purpose [47,49]. This system provides removing the small amount of impurities and any water from the solvent. An example of a solvent still is shown in figure 2.8.

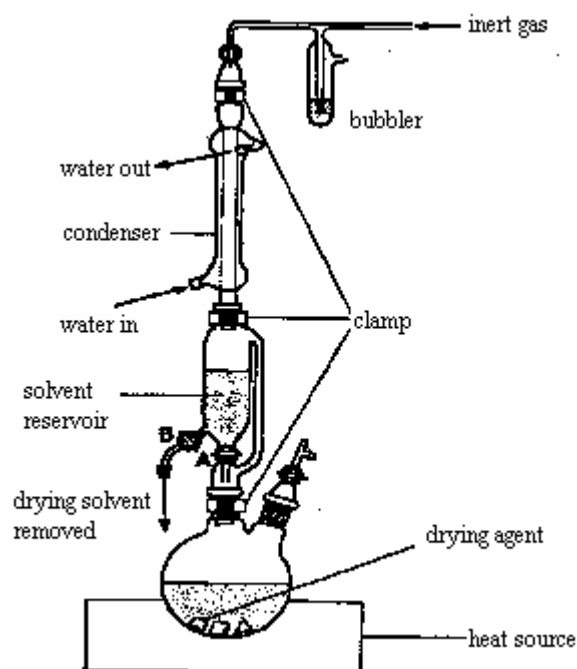


Figure 2.8. Solvent Still

It consists of a large distillation flask, connected to a reflux condenser via a piece of glassware which can simply be a pressure equalizing funnel modified by the inclusion of a second stopcock. Since the production of very dry solvents usually requires the exclusion of air from the apparatus, the still is fitted so that it can be operated under an inert atmosphere. Firstly, drying agent and solvent are added to the distillation flask under N_2 . With the stopcock A open, the solvent simply refluxes over the drying agent. When the stopcock A is closed, the solvent vapor passes up the narrow tube and dry solvent collects in the central piece of the apparatus. When the required volume of the solvent has been collected, it can be run off through the stopcock B. The solvents were prepared for the use as described below.

Toluene: The solvent is refluxed over calcium hydride and distilled and then stored onto 4A molecular sieves.

Dichloromethane: The same procedure is performed in purification of toluene.

Hexane: The solvent is readily dried by distilling and standing over 4A molecular sieves.

Tetrahydrofuran: The sodium wire and benzophenone are added to the solvent and it is refluxed under inert atmosphere until the deep blue color persists and then the solvent is distilled and stored onto 4A molecular sieves.

2.5. Experimental

All reactions, synthetic operations, and manipulations were carried out under an oxygen free and water free nitrogen atmosphere using standard schlenk techniques, a high-vacuum/gas double line manifold. Reactions were monitored by thin layer chromatography (TLC). Dinitrogen was obtained directly from a pressurized liquid nitrogen transfer/storage dewar. Solvents were dried by standard procedures, distilled and kept under nitrogen over 4A molecular sieves. All glassware was oven dried at 120 °C and schlenk ware was further purged by repeated evacuation and inert gas flushes prior to use. The new compounds were usually purified by column chromatography using silica gel 60 (70-230 mesh) with CH_2Cl_2 / n-Hexane mixture as eluant.

Reagents: Methoxy, ethoxy and, propoxy group functionalized anilines were obtained from Aldrich. Aniline was obtained from J.T.Baker. Triethylamine and tetrahydrofuran were obtained from Merck. Dichloromethane hexane, and toluene were obtained from Riedel. Acetonitrile and 1,2-dichloroethane were obtained from Panreac. Molybdenum pentachloride was obtained from Alfa Aesar. The starting material $[\text{MoTp}^*(\text{O})\text{Cl}_2]$, was prepared by standard procedures [35]. All yields are based on the starting material containing compound.

Instruments: Infrared spectra were recorded on a Magna IR spectrophotometer included diffuse reflectance accessory. $^1\text{H-NMR}$ spectra were recorded in CDCl_3 on 400 MHz High Performance Digital F.T.-N.M.R. at TUBITAK (Research Council of Turkey) and Varion AS 400 Mercury Plus at Ege University. Mass spectra analyses were performed on Joel AX505 FAB device using Xe at 3KV positive ion matrix m

NBA (meta-nitrobenzyl alcohol). The crystal structure determination was done by using a Bruker SMART CCD area-detector diffractometer.

2.6. Synthesis

2.6.1. [MoTp*(O)Cl](m-O)[MoTp*(Cl)(^oNC₆H₄OMe)] (1)

A mixture of [MoTp*(O)Cl₂] (0.3 g, 0.60 mmol), 4-methoxy aniline (0.14 g, 1.20 mmol) and dry Et₃N (0.6 cm³, 0.42 mmol) in dry toluene (20 cm³) was heated to reflux with stirring under N₂ for *ca.* 14 hour. During which time the solution became dark red-brown in colour. The mixture was cooled, filtered and evaporated to dryness. The residue was dissolved in dichloromethane and chromatographed on silica gel using CH₂Cl₂/n-hexane (9:1, v/v) as eluant. The red-brown fraction was collected, recrystallised from CH₂Cl₂/n-hexane to afford the compound [MoTp*(O)Cl](μ-O)[MoTp*(Cl)(≡NC₆H₄OMe)], as dark red microcrystals, yield 0.15 g (51%).

2.6.2. [MoTp*(O)Cl](m-O)[MoTp*(Cl)(^oNC₆H₄OEt)] (2)

A mixture of [MoTp*(O)Cl₂] (0.2 g, 0.40 mmol), 4-etoxy aniline (0.11 g, 0,81 mmol) and dry Et₃N (0.6 mL, 0.42 mmol) in dry toluene (20 cm³) was heated to reflux with stirring under N₂ for 21 hour. The reaction was fallowed by tlc using the procedure described above for (1) to afford the compound [MoTp*(O)Cl](μ-O)[MoTp*(Cl)(≡NC₆H₄OEt)] as red microcrystals, yield 0,09 g (45%).

2.6.3. [MoTp*(O)Cl](m-O)[MoTp*(Cl)(^oNC₆H₄OPr)] (3)

A mixture of [MoTp*(O)Cl₂] (0.2 g, 0.40 mmol), 4-propoxy aniline (0.12 g, 0,81 mmol) and dry Et₃N (0.6 mL, 0.42 mmol) in dry toluene (20 cm³) was heated to reflux with stirring under N₂ for 19 hour. The reaction was fallowed by tlc using the procedure described above for (1) to afford the compound [MoTp*(O)Cl](μ-O)[MoTp*(Cl)(≡NC₆H₄OPr)] as red microcrystals, yield 0,075 g (38%).

2.6.4. [MoTp*(O)Cl](m-O)[MoTp*(Cl)(^oNC₆H₄NO₂)] (4)

A mixture of [MoTp*(O)Cl₂] (0.3 g, 0.60 mmol), 4-nitro aniline (0.16 g, 1.21 mmol) and dry Et₃N (0.6 mL, 0.42 mmol) in dry toluene (20 cm³) was heated to reflux with stirring under N₂ for 16 hour. During which time the solution became dark brown in colour. The mixture was cooled, filtered and evaporated to dryness. The residue was dissolved in dichloromethane and chromatographed on silica gel using CH₂Cl₂/n-hexane (8:2, v/v) as eluant. The brown fraction was collected, recrystallised from CH₂Cl₂/n-hexane to afford the compound [MoTp*(O)Cl](μ-O)[MoTp*(Cl)(≡NC₆H₄NO₂)] as brown microcrystals, yield 0.12 g (40%).

2.6.5. [MoTp*(O)Cl](m-O)[MoTp*(O)(Cl)] (5)

A mixture of [MoTp*(O)Cl₂] (0.2 g, 0.40 mmol), aniline (0.076 g, 0.81 mmol) and dry Et₃N (0.6 cm³, 0.42 mmol) in dry toluene (20 cm³) was heated to reflux with stirring under N₂ for *ca.* 27 hour. During which time the solution became dark red-brown in colour. The mixture was cooled, filtered and evaporated to dryness. The residue was dissolved in dichloromethane and chromatographed on silica gel using CH₂Cl₂/n-hexane (7:3, v/v) as eluant. The maroon/red fraction was collected, recrystallised from CH₂Cl₂/n-hexane to afford the compound [MoTp*(O)Cl](μ-O)[MoTp*(O)(Cl)], as dark red microcrystals, yield 0,052 g (26 %)

CHAPTER 3

RESULT AND DISCUSSION

3.1. Synthetic Studies

In earlier studies with complexes containing the $[\text{MoTp}^*(\text{NO})\text{Cl}]$ fragment, it was found that reaction of the 16 electron [diamagnetic, formally Mo(II)] complex $[\text{MoTp}^*(\text{NO})\text{Cl}_2]$ with aromatic amines in the presence of Et_3N results in displacement of one chlorine ion by a deprotonated amide ion to give the products $[\text{MoTp}^*(\text{NO})\text{Cl}(\text{NHR})]$ [27]. It was known that in different oxidation states, both the nitrosylmolybdenum (I) and oxomolybdenum (V) centres behave very similarly. This is because (i) they both have an unpaired electron in a d_{xy} orbital and (ii) the strong p-electron-withdrawing in effect of the nitrosyl group on Mo^{I} and the strong p-electron-donating effect of the oxo group on Mo^{V} , means that the electron density on each type of metal centre is actually quite similar, and the large difference in oxidation states is more apparent than real.[50] Therefore we were interested to see if the reaction of $[\text{MoTp}^*(\text{O})\text{Cl}_2]$ with aromatic amines followed a similar course as $[\text{MoTp}^*(\text{NO})\text{Cl}_2]$

Reaction of $[\text{MoTp}^*(\text{O})\text{Cl}_2]$, $\text{Tp}^*(\text{Hydrotris}(3,5\text{-dimethyl pyrazol-1-yl borato)})$ and aromatic p-substituted anilines $\text{H}_2\text{NC}_6\text{H}_4\text{R}$ ($\text{R} = \text{OMe}, \text{OEt}, \text{OPr}, \text{NO}_2$) in the presence of triethylamine in toluene produced the novel dinuclear oxo-bridged oxo(arylimido) molybdenum (V) complexes. $[\text{MoTp}^*(\text{O})\text{Cl}](\mu\text{-O})[\text{MoTp}^*\text{Cl}(\equiv\text{NC}_6\text{H}_4\text{R})]$ ($\text{R} = \text{OMe}, \text{OEt}, \text{OPr}, \text{NO}_2$). The structure of $[\text{MoTp}^*(\text{O})\text{Cl}](\mu\text{-O}) [\text{MoTp}^*\text{Cl}(\equiv\text{NC}_6\text{H}_4\text{OMe})]$ was determined by X-ray diffraction method.

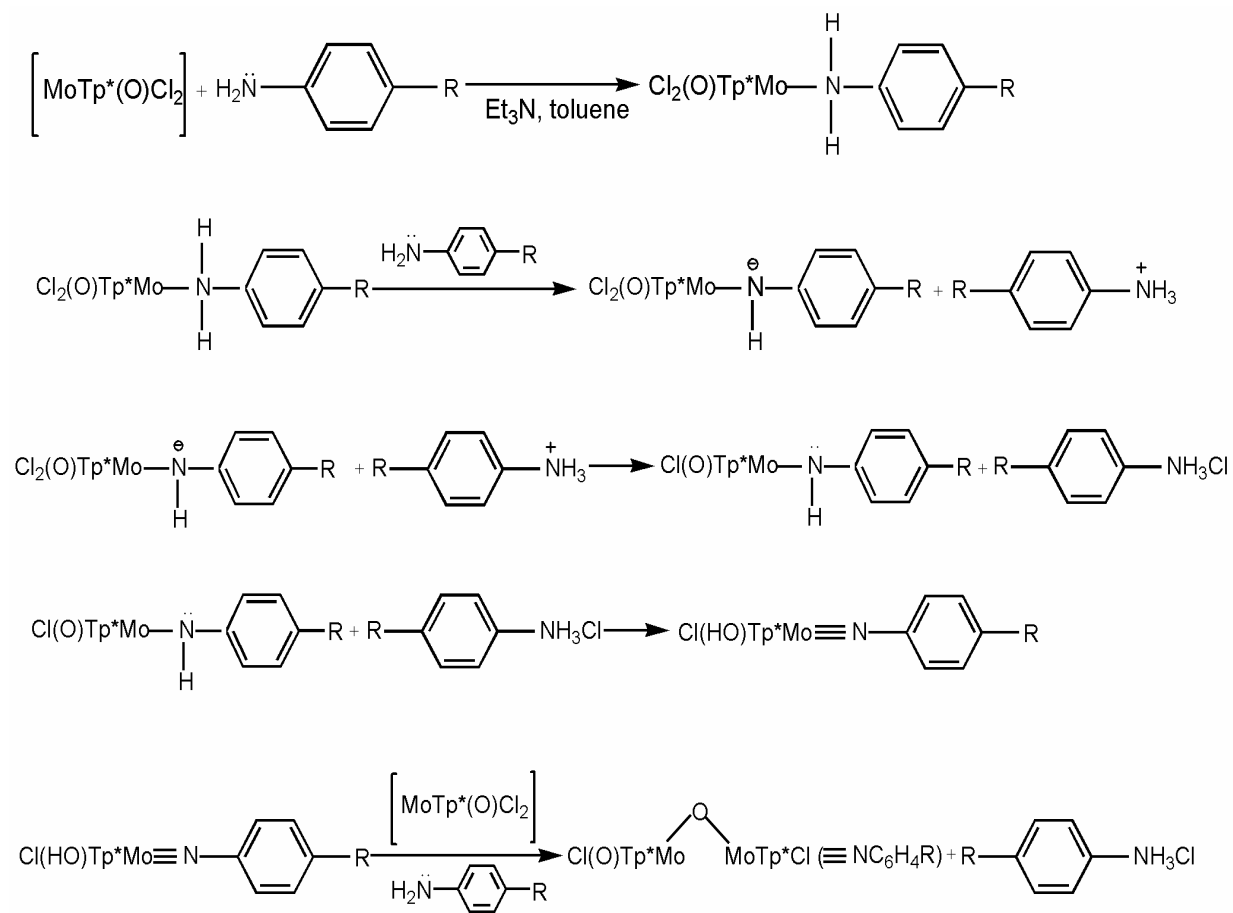
Surprisingly the reaction of $[\text{MoTp}^*(\text{O})\text{Cl}_2]$ and aniline in the presence of triethylamine in toluene produced binuclear oxo-bridged molybdenum (V) compound $[\text{MoTp}^*(\text{O})\text{Cl}]_2(\mu\text{-O})$. The previously reported compounds having Mo-O-Mo linkage and tris(pyrazolylborate) co-ligand were prepared by completely different methods. For example, a number of dinuclear oxo-bridged Mo(V) compounds with tris(pyrazolborate) co-ligand were produced by various combinations of oxygen atom transfer, comproportionation, aquation and hydrolysis reactions at Mo(VI) or Mo(V).

For example; it was mentioned before, McCleverty et. al.[44] prepared the compound $[\text{MoTp}^*(\text{O})\text{Cl}]_2(\mu\text{-O})$ by the reaction of $[\text{MoTp}^*(\text{O})_2\text{Cl}]$ and PPh_3 in wet toluene containing approximately 0.03% water. Millar et.al.[43] prepared the same compound by treatment of 1,3-dimethoxy-para-tert-butylcalix(4)arene and $[\text{MoTp}^*(\text{O})\text{Cl}]$ in toluene with reflux. The synthesis was successful in the absence of calixarene as well and it was suggested that the complex was formed due to the presence of adventitious water. The syntheses of geometric isomers of $[\text{MoTp}(\text{O})\text{Cl}]_2(\mu\text{-O})$ (Tp = hydrotris pyrazolylborate) were accomplished in aqueous media: The cis (C_2) isomer of $[\text{MoTp}(\text{O})\text{Cl}]_2(\mu\text{-O})$ was prepared by the reaction of Tp with MoOCl_5^{2-} and the related trans (C_i) isomer was obtained by the treatment of $\text{MoTp}(\text{Cl})_3$ with $\text{H}_2\text{O}/\text{CH}_2\text{Cl}_2$ mixture [34, 40]

The reactions were performed at reflux temperature over periods ranging from 14-27 h. Formation of the complexes was followed by thin layer chromatography (tlc) using CH_2Cl_2 / n-hexane (v:v, different ratios) as eluant. The products were readily purified by column chromatography on silice gel 60 (70-230 mesh) using the same solvent mixture as eluant. The complexes are air-stable and soluble in chlorinated solvents.

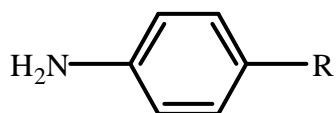
There is a number of synthetic methods known for introducing imido functionality into coordination compounds. In our work the preparation of the compounds (1)-(4) were accomplished by double deprotonation of the p-substituted anilines. This is well known [23] synthetic methodology for the preparation of organoimido complexes of Mo(V) and Mo(VI) in which organic compounds are employed as the imido transfer reagent. Despite the steric barrier provided by the 3-methyl groups of Tp^* ligand, the formation of the Mo-O-Mo linkage in (1)-(4) is interesting. It could be suggested that compounds (1)-(4) were formed by treating $[\text{MoTp}^*(\text{O})_2\text{Cl}]$ with p-substituted anilines, each of which undergoes double deprotonation to yield the mononuclear species $[\text{MoTp}^*(\text{O})\text{Cl}(\text{H}_2\text{NC}_6\text{H}_4\text{R})]$, $[\text{MoTp}^*(\text{O})\text{Cl}(\text{HNC}_6\text{H}_4\text{R})]$, and $[\text{MoTp}^*(\text{O})\text{Cl}(\equiv\text{NC}_6\text{H}_4\text{R})]$ (R =, OMe, OEt, OPr, NO_2), as subsequent intermediates. The mononuclear imido species, $[\text{MoTp}^*(\text{O})\text{Cl}(\equiv\text{NC}_6\text{H}_4\text{R})]$, further reacts with unreacted starting material to form the oxo-bridged dimetallic oxo (arylimido) molybdenum (V) compounds $[\text{MoTp}^*(\text{O})\text{Cl}](\mu\text{-O}) [\text{MoTp}^*\text{Cl}(\equiv\text{NC}_6\text{H}_4\text{R})]$

The following synthetic route for the formation of novel compounds (1)-(4) could be suggested.



Scheme 3.1. Synthetic route for the formation novel compounds $[\text{MoTp}^*(\text{O})\text{Cl}](\mu\text{-O})$
 $[\text{MoTp}^*\text{Cl}(\equiv\text{NC}_6\text{H}_4\text{R})](1)-(4)$ ($\text{R} =, \text{OMe}, \text{OEt}, \text{OPr}, \text{NO}_2$),

Meta-substituted aromatic ligands are less effective at mediating electronic interactions than their para-substituted analogues [51]. Therefore in all our reactions para-substituted anilines were preferred.



($\text{R} : \text{H}, \text{NO}_2, \text{OMe}, \text{OEt}, \text{OPr}$)

Figure 3.1. The Structures of p-Functionalized Anilines

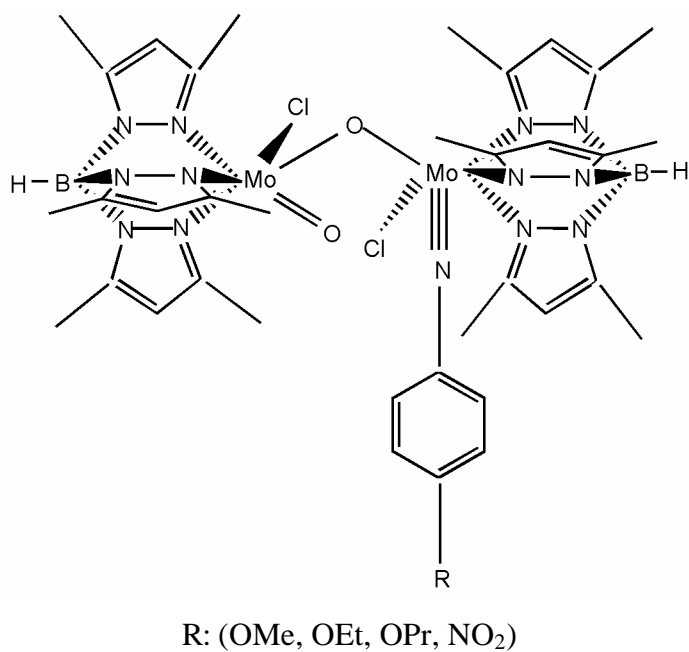


Figure 3.2. The structures for the complexes (1), (2), (3), (4)

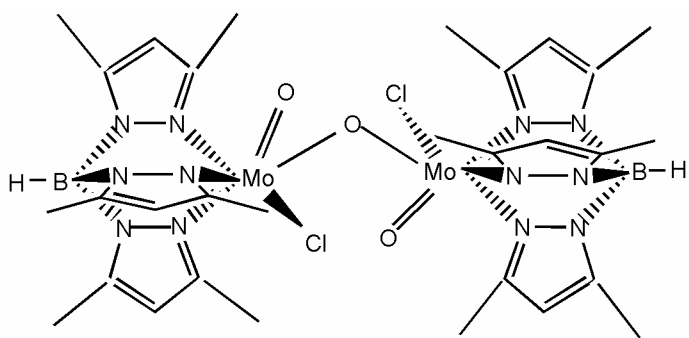


Figure 3.3. The structure for the complex (5)

3.2. Crystallographic Studies

3.2.1. Crystal Structure Determination and Refinement

A single crystal of $[\text{MoTp}^*(\text{O})\text{Cl}](\mu\text{-O})[\text{MoTp}^*(\text{Cl})(\equiv\text{NC}_6\text{H}_4\text{OMe})]$ was recrystallized from CH_2Cl_2 /hexane mixture and coated in high-vacuum grease and mounted on a glass fibre. A view of the molecular structure of $[\text{MoTp}^*(\text{O})\text{Cl}](\mu\text{-O})[\text{MoTp}^*(\text{Cl})(\equiv\text{NC}_6\text{H}_4\text{OMe})]$ along with the atomic labelling scheme is shown in Figure 3.5. X-ray measurements were made using a Bruker SMART CCD area-detector diffractometer with $\text{Cu-K}\alpha$ radiation ($\lambda = 1.54184 \text{ \AA}$) [52]. Intensities were integrated [53] from several series of exposures, each exposure covering 0.3° in ω , and the total data set being a sphere. Absorption corrections were applied, based on multiple and symmetry-equivalent measurements [54]. The structure was solved by Patterson synthesis and refined by least squares on weighted F^2 values for all reflections (Table 3.1) [55]. All non-hydrogen atoms were assigned anisotropic displacement parameters and refined without positional constraints. Hydrogen atoms H(1A), H(2A) were located in the electron density difference map, assigned isotropic displacement parameters and refined without positional constraints. All other hydrogen atoms were constrained to ideal geometries and refined with fixed isotropic displacement parameters. Refinement proceeded smoothly to give the residuals shown in Table 3.1. Complex neutral-atom scattering factors were used [56].

Table 3.1. Crystal data and structure refinement for [MoTp*(O)Cl](μ -O)[MoTp*Cl($^{\circ}$ NC₆H₄OMe)]

Empirical Formula	C ₃₇ H ₅₁ B ₂ Cl ₂ Mo ₂ N ₁₃ O ₃
Formula Weight	1010.31
Temperature	100(2) K
Wavelength	1.54184 Å
Crystal system	Triclinic
Space group	P-1
Unit cell dimension	a = 11.0200 (2) Å a = 77.3320 (10) ^o b = 11.5868 (2) Å b = 76.8440 (10) ^o c = 18.7414 (3) Å ? = 75.8450 (10) ^o
Volume	2225.27 (7) Å ³
Z	2
Density (calculated)	1.508 Mg/m ³
Absorption coefficient	0.735 mm ⁻¹
F (000)	1032
Crystal size	0.08x0.08x0.03 mm
? range for data collection	1.13 to 25.70 ^o
Index ranges	-13<=h<=12, -13<=k<=14, -22<=l<=20
Reflections collected	15997
Independent reflections	7504 [R _{int} = 0.0226]
Completeness to ? = 25.70 ^o	88.7 %
Refinement method	Full-matrix least-squares on F ²
Data/restraints/parameters	7504/0/553
Goodness-of-fit F2	S = 0.924
R indices [for 6435 reflections with I>2s(I)]	R ₁ = 0.0227, wR ₂ = 0.0533
R indices (for all 7504 data)	R ₁ = 0.267, wR ₂ = 0.0540
Weighing scheme	w ⁻¹ = s ² (F _o ²) + (aP) ² + bP where P = [max(F _o ² , 0) + 2F _c ²]/3 A = 0.00316, b = 0.0000
Largest diff. Peak and hole	0.375 and -0.489 eÅ ⁻³

3.2.2. Crystal Structure of $[\text{MoTp}^*(\text{O})\text{Cl}](\mu\text{-O})[\text{MoTp}^*(\text{Cl})(\text{C}\equiv\text{NC}_6\text{H}_4\text{OMe})]$

The compound $[\text{MoTp}^*(\text{O})\text{Cl}](\mu\text{-O})[\text{MoTp}^*(\text{Cl})(\text{C}\equiv\text{NC}_6\text{H}_4\text{OMe})]$ is comprised of two unidentical MoTp^*Cl unit connected by a single oxo bridge. There are two pseudo-octahedral metal centers with three nitrogen atoms of the Tp^* ligand occupying one face of the octahedron (Figure 3.4.).

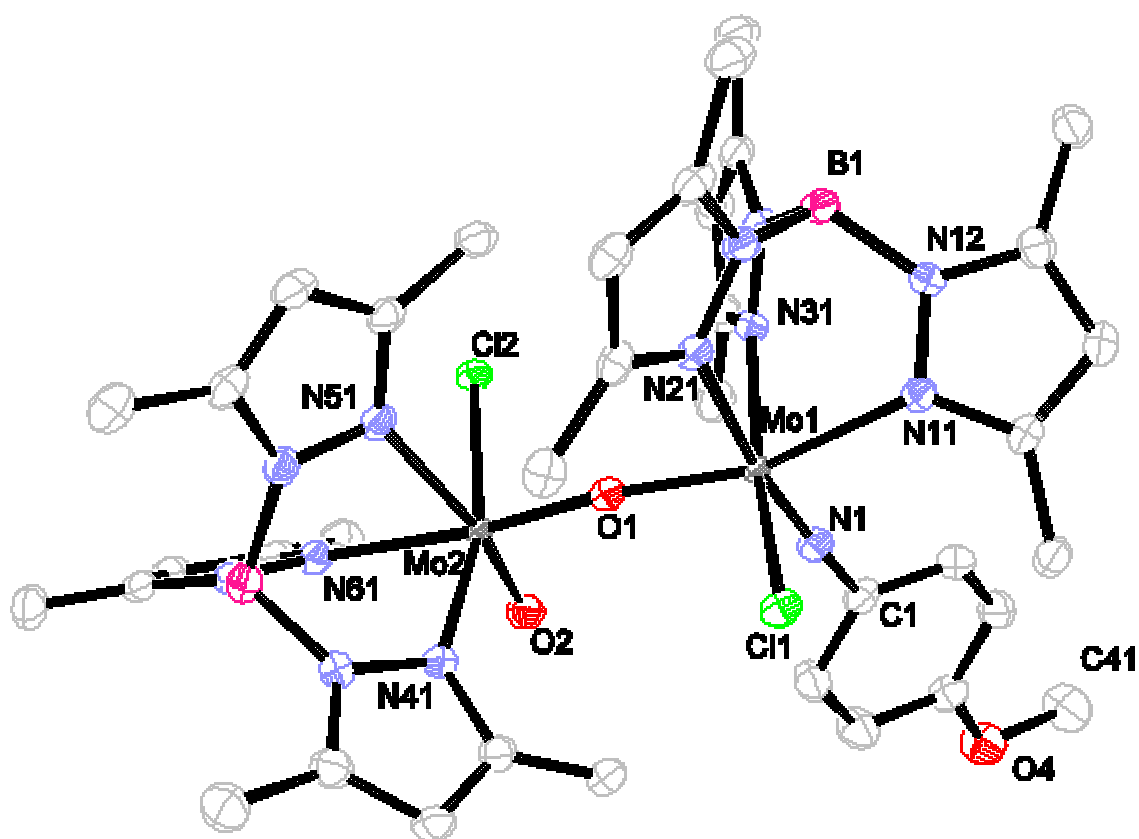


Figure 3.4. Crystal Structure of $[\text{MoTp}^*(\text{O})\text{Cl}](\mu\text{-O})[\text{MoTp}^*(\text{Cl})(\text{C}\equiv\text{NC}_6\text{H}_4\text{OMe})]$

Table 3.2. Selected bond lengths (Å) and angles (°) for [MoTp*(O)Cl](μ-O)[MoTp*(Cl)(≡NC₆H₄OMe)]

Mo(1)-N(1)	1.7391(19)
Mo(1)-O(1)	1.9004(14)
Mo(1)-Cl(1)	2.4159(5)
O(1)-Mo(2)	1.8731(14)
N(1)-C(1)	1.381(3)
Mo(2)-O(2)	1.6779(16)
Mo(2)-Cl(2)	2.3918(5)
B(1)-N(22)	1.522(3)
B(1)-N(12)	1.544(3)
B(1)-N(32)	1.546(3)
B(2)-N(52)	1.525(3)
B(2)-N(42)	1.547(3)
B(2)-N(62)	1.546(3)
Mo(1)-N(11)	2.2185(17)
Mo(1)-N(21)	2.2768(18)
Mo(1)-Cl(1)	2.4159(5)
Mo(2)-N(41)	2.1600(18)
Mo(2)-N(61)	2.2180(17)
Mo(2)-N(51)	2.3811(18)
Mo(2)-O(1)-Mo(1)	164.99(9)
C(1)-N(1)-Mo(1)	176.67(7)
N(1)-Mo(1)-O(1)	100.16(7)
N(1)-Mo(1)-N(11)	93.09(7)
N(1)-Mo(1)-Cl(1)	97.03(6)
O(1)-Mo(1)-Cl(1)	98.45(5)
N(11)-Mo(1)-Cl(1)	88.19(5)
O(2)-Mo(2)-O(1)	101.60(7)
O(1)-Mo(2)-N(41)	92.23(7)
O(2)-Mo(2)-Cl(2)	98.93(5)
O(1)-Mo(2)-Cl(2)	95.32(5)
N(31)-Mo(1)-N(11)	81.70(7)
N(41)-Mo(2)-N(61)	82.96(7)
O(2)-Mo(2)-N(51)	169.67(7)
O(1)-Mo(2)-N(51)	88.30(6)
N(41)-Mo(2)-N(51)	82.27(7)
N(61)-Mo(2)-N(51)	78.69(6)
O(2)-Mo(2)-N(61)	91.26(7)
O(1)-Mo(2)-N(61)	166.60(7)
N(41)-Mo(2)-N(61)	82.96(7)

Mo(2) is coordinated by facial Tp*, terminal oxo, chloro and bridging oxo ligand whereas the Mo(1) is coordinated by facial Tp*, chloro, arylimido and a bridging oxo ligand. The two chloride atoms were trans to each other. Selected bond distances and bond angles are given in Table 3.2. and atomic co-ordinates are presented in Table 3.3 and The Mo(1)-O(1), Mo(2)-O(1), Mo(2)-O(2), Mo(1)-Cl(1), Mo(2)-Cl(2), distances of 1.9004(14), 1.8731(14), 1.6779(16), 2.4159(5), 2.3918(5), (Å), respectively, are all within respected ranges [56]. The Mo(1)-(μ-O) distance was reported [44] as 1.8886(9) (Å) in $[\{\text{MoTp}^*(\text{O})\text{Cl}\}_2](\mu\text{-O})$. The X-ray crystal structures of two geometric isomers of the related complex $[\text{MoTp}(\text{O})\text{Cl}]_2(\mu\text{-O})$ (Tp = hydrotrispyrazolborate) were reported by Lincoln and Koch. The reported bond distances are comparable to those encountered here. For instance, in the trans isomer, the Mo(1)-(μ-O) distances of 1.861(1) Å is reported [34] which is comparable to the above value for $\text{MoTp}^*(\text{O})\text{Cl}(\mu\text{-O})[\text{MoTp}^*(\text{Cl})(\equiv\text{NC}_6\text{H}_4\text{OMe})]$.

For $[\text{MoTp}^*(\text{O})\text{Cl}](\mu\text{-O})[\text{MoTp}^*(\text{Cl})(\equiv\text{NC}_6\text{H}_4\text{OMe})]$, deviations from octahedral geometry are manifest in the bond angles O(2)-Mo(2)-O(1) ($101.60(7)^\circ$) and O(1)-Mo(1)-N(11) ($164.28(7)^\circ$). These values are in accord with the data reported for $[\text{MoTp}^*\text{OCl}]_2(\mu\text{-O})$ and $[\text{MoTp}^{\text{Pr}}\text{OCl}](\mu\text{-O})[\text{MoTp}^{\text{Pr}}\text{O}(\text{OH})]$ [42]. The Mo(1)-O(1)-Mo(2) angle of $164.99(9)^\circ$ deviates considerably from linearity (cf. $177.4(4)^\circ$ for (cis) $[\text{MoTp}^*(\text{O})\text{Cl}]_2(\mu\text{-O})$ and $177.3(2)^\circ$ and 180° for (trans) $[\text{MoTp}(\text{O})\text{Cl}]_2(\mu\text{-O})$ [34]. This value is comparable to the one ($158.5(2)^\circ$) reported [42] for the compound $[\text{MoTp}^{\text{Pr}}\text{OCl}](\mu\text{-O})[\text{MoTp}^{\text{Pr}}\text{O}(\text{OH})]$ $176.67(17)$.

Molybdenum nitrogen multiple bond could either be a double bond with Mo-N-C angle of 120° or a triple bond with Mo-N-C angle of 180° . In the first case imido group acts as a four electron donor with no lone pair in the latter case it behaves as a six electron donor.

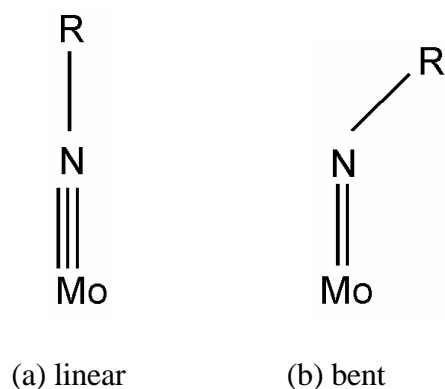


Figure 3.5. Linear (a) and bent (b) imido linkages

The Mo(1)-N(1)-C(1) bond angle of $176.67(17)^\circ$ for $[\text{MoTp}^*(\text{O})\text{Cl}](\mu\text{-O})[\text{MoTp}^*(\text{Cl})(\equiv\text{NC}_6\text{H}_4\text{OMe})]$ is indicative of a linear Mo-N-C(aryl) unit. The typical range for this arrangement was reported as $160\text{-}180^\circ$ [57]. Mo(1)-N(1) bond length of $1.7391(19) \text{ \AA}$ is also indicative of a Mo \equiv N bond. This value is in accord with the reported bond length values for compounds containing Mo=N bond and shorter than the Mo=N ones [58].

Table 3.3. Atomic coordinates ($\times 10^4$) and equivalent isotropic displacement parameters ($\text{\AA}^2 \times 10^3$) for K1m. $U(\text{eq})$ is defined as one third of the trace of the orthogonalized U_{ij} tensor.

	x	y	z	U (eq)		x	y	z	U (eq)
Mo(1)	1997(1)	3127(1)	2070(1)	12(1)	C(34)	5334(2)	1176(2)	731(1)	26(1)
N(1)	2941(2)	3327(2)	2643(1)	21(1)	C(35)	4726(2)	1532(2)	1408(1)	23(1)
C(1)	3746(2)	3494(2)	3062(1)	22(1)	C(36)	4747(2)	1787(2)	-595(1)	30(1)
C(2)	4635(2)	4220(2)	2751(1)	26(1)	C(37)	5171(2)	1169(2)	2136(1)	28(1)
C(3)	5461(2)	4362(2)	3164(1)	26(1)	Mo(2)	1835(1)	-22(1)	3065(1)	13(1)
C(4)	5372(2)	3810(2)	3910(1)	26(1)	Cl(2)	3586(1)	-940(1)	2217(1)	22(1)
C(5)	4478(2)	3082(2)	4226(1)	31(1)	O(2)	2622(2)	32(1)	3721(1)	24(1)
C(6)	3683(2)	2911(2)	3806(1)	28(1)	B(2)	-729(3)	-1292(2)	3445(2)	23(1)
O(4)	6096(2)	3932(2)	4375(1)	33(1)	N(41)	-25(2)	464(2)	3734(1)	19(1)
C(41)	7081(3)	4585(3)	4071(2)	41(1)	N(42)	-970(2)	-166(2)	3814(1)	21(1)
Cl(1)	9(1)	4261(1)	2649(1)	23(1)	C(43)	-1995(2)	307(2)	4287(1)	26(1)
O(1)	1736(1)	1544(1)	2512(1)	20(1)	C(44)	-1704(2)	1229(2)	4528(1)	26(1)
B(1)	2642(3)	3622(2)	229(1)	22(1)	C(45)	-463(2)	1300(2)	4179(1)	23(1)
N(11)	2279(2)	4806(2)	1275(1)	20(1)	C(46)	-3216(2)	-143(2)	4489(2)	36(1)
N(12)	2724(2)	4728(2)	536(1)	19(1)	C(47)	345(2)	2084(2)	4290(1)	26(1)
C(13)	3137(2)	5740(2)	172(1)	22(1)	N(51)	615(2)	-414(2)	2280(1)	21(1)
C(14)	2926(2)	6503(2)	678(1)	24(1)	N(52)	-432(2)	-926(2)	2601(1)	22(1)
C(15)	2393(2)	5899(2)	1363(1)	21(1)	C(53)	-967(2)	-1115(2)	2065(1)	25(1)
C(16)	3738(2)	5897(2)	-636(1)	26(1)	C(54)	-275(2)	-706(2)	1389(1)	26(1)
C(17)	1962(2)	6345(2)	2087(1)	26(1)	C(55)	711(2)	-287(2)	1539(1)	22(1)
N(21)	846(2)	3041(2)	1224(1)	20(1)	C(56)	-2084(2)	-1710(2)	2241(2)	31(1)
N(22)	1301(2)	3376(2)	477(1)	20(1)	C(57)	1743(2)	215(2)	983(1)	26(1)
C(23)	464(2)	3294(2)	72(1)	24(1)	N(61)	1596(2)	-1886(2)	3583(1)	20(1)
C(24)	-548(2)	2895(2)	566(1)	24(1)	N(62)	440(2)	-2209(2)	3693(1)	21(1)
C(25)	-290(2)	2755(2)	1280(1)	23(1)	C(63)	563(2)	-3399(2)	3980(1)	24(1)
C(26)	667(2)	3627(2)	-753(1)	29(1)	C(64)	1806(2)	-3839(2)	4069(1)	24(1)
C(27)	-1116(2)	2369(2)	2002(1)	27(1)	C(65)	2430(2)	-2873(2)	3816(1)	22(1)
N(31)	3651(2)	2342(2)	1306(1)	19(1)	C(66)	-522(3)	-4033(2)	4148(1)	31(1)
N(32)	3591(2)	2531(2)	565(1)	20(1)	C(67)	3791(2)	-2873(2)	3805(1)	28(1)
C(33)	4596(2)	1811(2)	209(1)	24(1)					

3.3. Spectroscopic studies

The $^1\text{H-NMR}$ spectra data for the complexes are given in tables 3.5-3.9 and their spectra are shown in figures 3.7, 3.9, 3.11, 3.13, 3.15.

The $^1\text{H-NMR}$ spectra of the new complexes $[\text{MoTp}^*(\text{O})\text{Cl}](\mu\text{-O})[\text{MoTp}^*(\text{Cl})(\equiv\text{NC}_6\text{H}_4\text{R})]$ ($\text{R} = \text{OMe}, \text{OEt}, \text{OPr}, \text{NO}_2$) and $[\text{MoTp}^*(\text{O})\text{Cl}]_2(\mu\text{-O})$ are consistent with the formulation of them. They exhibited all the expected peaks.

The four C_6H_4 protons are clearly split into two sets of two (implying the equivalence of H^2 with H^6 , and H^3 with H^5 , by free rotation of the phenyl ring with respect to the metal core). The signals attributable to the Tp^* ligand appeared as two groups of singlets in the region 2.29-3.17 p.p.m. assigned to the pyrazolyl ring methyl protons and 5.36 -6.02 p.p.m. due to the pyrazolyl ring C^4 protons. The low symmetry of new compounds means that all three pyrazol C^4 protons and all six methyl groups of the Tp^* ligand are inequivalent. For $[\text{MoTp}^*(\text{O})\text{Cl}](\mu\text{-O})[\text{MoTp}^*(\text{Cl})(\equiv\text{NC}_6\text{H}_4\text{R})]$ ($\text{R} = \text{OMe}, \text{OEt}, \text{OPr}$) six pyrazolyl C^4 signals were observed in the range δ 6.02-5.36 due to the two inequivalent Tp^* ligand whereas in the spectrum of $[\text{MoTp}^*(\text{O})\text{Cl}](\mu\text{-O})[\text{MoTp}^*(\text{Cl})(\equiv\text{NC}_6\text{H}_4\text{NO}_2)]$ two signals were observed. The reason for observing two resonances instead of six in $[\text{MoTp}^*(\text{O})\text{Cl}](\mu\text{-O})[\text{MoTp}^*(\text{Cl})(\equiv\text{NC}_6\text{H}_4\text{NO}_2)]$ could be attributed to accidental degeneracy of the three C^4 resonances in two inequivalent Tp^* ligands. This effect has previously been observed by McCleverty et al [59,60]. The low symmetry of these compounds also means six methyl resonances for each Tp^* ligand must be observed in the area of 1.5-3.5 p.p.m. Indeed, six resonances attributable to the methyl groups of Tp^* ligand were observed for the compounds $[\text{MoTp}^*(\text{O})\text{Cl}](\mu\text{-O})[\text{MoTp}^*(\text{Cl})(\equiv\text{NC}_6\text{H}_4\text{R})]$ ($\text{R} = \text{OMe}, \text{OEt}, \text{OPr}$) and $[\text{MoTp}^*(\text{O})\text{Cl}](\mu\text{-O})[\text{MoTp}^*(\text{Cl})(\equiv\text{NC}_6\text{H}_4\text{NO}_2)]$ in the region δ 3.20-2.29 and δ 2.71-2.12 respectively. The observation of only six resonances (total integrated area equivalent to twelve protons) instead of twelve could also be attributed to accidental degeneracy of six methyl resonances of two inequivalent Tp^* ligands.

Generally NH_2 and NH protons appear in the range δ 11.14-13.15 p.p.m. [61]. No broad signals typical of amine or amide protons were observed in the $^1\text{H-NMR}$ spectra of the new compounds which leads us to believe that are either $\text{Mo}=\text{N}$ or $\text{Mo}\equiv\text{N}$ linkages.

Further support for the formulations of these complexes is provided by the FT-IR spectrometry. FT-IR spectra data for the complexes are given in table 1.2 and their spectra are shown in figure 3.6, 3.8, 3.10, 3.12, 3.14. All complexes exhibit the expected absorptions due to the Tp* ligand (ca. 2500 cm⁻¹ due to $\nu_{\text{(BH)}}$ and 1400 cm⁻¹ associated with the pyrazolyl ring). They possess bands characteristic of the terminal Mo=O unit (ca. 960 cm⁻¹). This value was reported as 964 cm⁻¹ for the starting material [MoTp*(O)Cl₂] [35]. For the compounds [MoTp(O)Cl₂](μ -O)(cis isomer), and [MoTp(O)Cl₂](μ -O) (trans isomer), the peak at 958 cm⁻¹ was assigned as Mo=O of the terminal oxo groups [34].

Table 3.4. FT-IR Data for the New Complexes

Complexes	$\nu_{\text{(BH)}}$	$\nu_{\text{(Mo=O)}}$	$\nu_{\text{(Mo=N)}}$
(1)	2548	957	1205
(2)	2547	949	1212
(3)	2547	949	1212
(4)	2547	961	1204
(5)	2547	960	1204

The compound [MoTp*(O)Cl]₂(μ -O) exhibited $\nu_{\text{(Mo=O)}}$ at 960 and 859 cm⁻¹. This value has been reported as 961 and 971 cm⁻¹ for [MoTp^{Pr}(O)Cl](μ -O)[MoTp^{Pr}(O)(OH)] (Tp^{Pr} = Hydrotris-(3-isopropylpyrazolyl)borate) [42]. The IR spectrum of the mixed valence compound, [Mo^(V)Tp*O₂](μ -O) [Mo^(VI)Tp*(O)Cl] exhibited three $\nu_{\text{(Mo=O)}}$ bands in the region 850-1000 cm⁻¹. The $\nu_{\text{(Mo=O)}}$ bands were assigned to Mo^(V)=O (955 cm⁻¹) and cis-Mo^(VI)O₂ (925, 895 cm⁻¹) [45]. A detailed infrared and raman spectroscopy study was carried out for the geometric isomers (cis and trans) of [MoTp(O)Cl₂](μ -O) [30]. According to this study, the peaks at 784 cm⁻¹ and 456 cm⁻¹ were assigned to the asymmetric stretch and the deformation mode of the linear oxo-bridged unit, respectively [40]. For the compound [MoTp*(O)Cl]₂(μ -O), symmetric stretch oxo-bridged unit was reported as 753 cm⁻¹ [35]. Therefore, the peaks observed for the new

compounds $[\text{MoTp}^*(\text{O})\text{Cl}](\mu\text{-O})[\text{MoTp}^*(\text{Cl})(\equiv\text{NC}_6\text{H}_4\text{R})]$ ($\text{R} = \text{OMe}, \text{OEt}, \text{OPr}, \text{NO}_2$) at ca. 755 cm^{-1} and 455 cm^{-1} could be assigned to asymmetric stretch and deformation mode of the Mo-O-Mo unit, respectively. The presence of the μ -oxo ligand was indicated by a strong, broad $\nu_{\text{as}}(\text{Mo-O-Mo})$ band at 750 cm^{-1} for the compound $[\text{Mo}^{(\text{V})}\text{Tp}^*\text{O}_2](\mu\text{-O})[\text{Mo}^{(\text{VI})}\text{Tp}^*(\text{O})\text{Cl}]$ [45] as well.

The two vibrations at ca. 3370 cm^{-1} and 3450 cm^{-1} from the symmetric and asymmetric stretching modes of the NH_2 groups of the free ligands have completely disappeared in the IR spectra of all the new complexes. Indeed, the structure determined for the compound $[\text{MoTp}^*(\text{O})\text{Cl}](\mu\text{-O})[\text{MoTp}^*(\text{Cl})(\equiv\text{NC}_6\text{H}_4\text{OMe})]$ by X-ray diffraction analyses revealed a triple bond between molybdenum and nitrogen. In general, identifying a $\nu_{(\text{Mo}=\text{N})}$ or $\nu_{(\text{Mo}\equiv\text{N})}$ vibration is a difficult task because of (i) the variability in the Mo-N bond order, and (ii) coupling of the Mo=N vibration to other vibrations in the molecule, in particular the adjacent N-C vibration of the imido group. However, a value of $1100\text{-}1300\text{ cm}^{-1}$ for the $\nu_{(\text{Mo}=\text{N})}$ has been suggested [56] and McCleverty et al. reported values in the range $1200\text{-}1250\text{ cm}^{-1}$ for the compounds $[\text{MoTp}^*(\text{O})\text{Cl}(=\text{NR})]$ ($\text{R} = 4\text{-tolyl}, \text{and } \text{C}_6\text{H}_4\text{NMe}_{2-4}$) [21]. The IR spectra of the oxo bridged oxo(arylimido) molybdenum(V) compounds, $[\text{MoTp}^*(\text{O})\text{Cl}](\mu\text{-O})[\text{MoTp}^*(\text{Cl})(\equiv\text{NC}_6\text{H}_4\text{R})]$, ($\text{R} = \text{OMe}, \text{OEt}, \text{OPr}, \text{NO}_2$) also exhibited peaks around $1200\text{-}1300\text{ cm}^{-1}$ range which may be ascribed to $\nu_{(\text{Mo}\equiv\text{N})}$. [27]

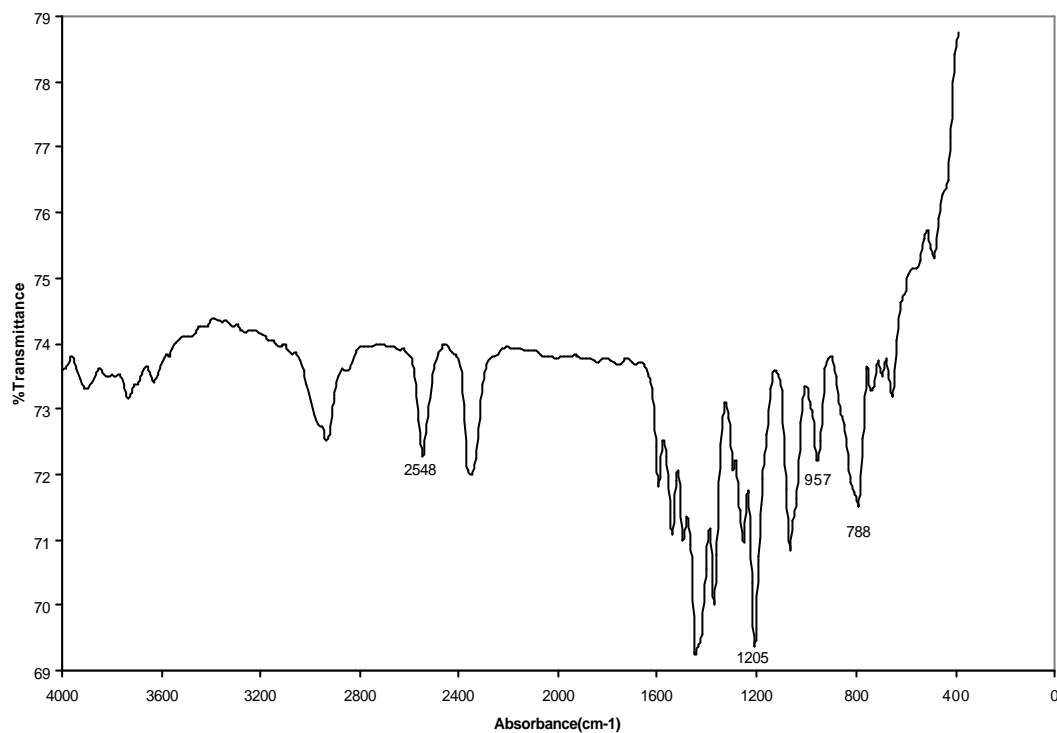


Figure 3.6. FT-IR spectrum of $[\text{MoTp}^*(\text{O})\text{Cl}](\mu\text{-O}) [\text{MoTp}^*\text{Cl}(\text{O}^\circ\text{NC}_6\text{H}_4\text{OMe})]$ (1)

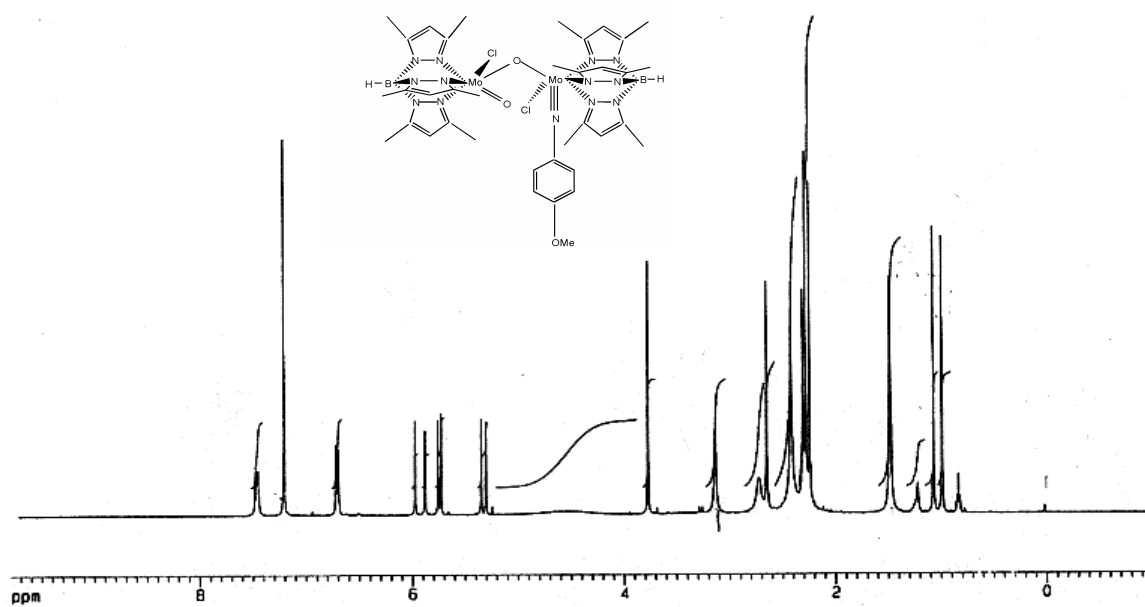


Figure 3.7. $^1\text{H-NMR}$ spectrum of $[\text{MoTp}^*(\text{O})\text{Cl}](\mu\text{-O}) [\text{MoTp}^*\text{Cl}(\text{O}^\circ\text{NC}_6\text{H}_4\text{OMe})]$ (1)

Table 3.5. ^1H -NMR data of $[\text{MoTp}^*(\text{O})\text{Cl}](\mu\text{-O}) [\text{MoTp}^*\text{Cl}(\text{}^o\text{NC}_6\text{H}_4\text{OMe})]$ (1)

A^c	$d^b/ \text{p.p.m}$	Assignment
2	7,53	d, $\text{NC}_6\text{H}_4\text{OMe}$ J(HH) 8
2	6,77	d, $\text{NC}_6\text{H}_4\text{OMe}$ J(HH) 8
1	6,04	s, $\text{Me}_2\text{C}_3\text{HN}_2$
1	5,94	s, $\text{Me}_2\text{C}_3\text{HN}_2$
1	5,82	s, $\text{Me}_2\text{C}_3\text{HN}_2$
1	5,79	s, $\text{Me}_2\text{C}_3\text{HN}_2$
1	5,41	s, $\text{Me}_2\text{C}_3\text{HN}_2$
1	5,36	s, $\text{Me}_2\text{C}_3\text{HN}_2$
3	3,83	s, OMe
36	3,20-2,30	s, $\text{Me}_2\text{C}_3\text{HN}_2$

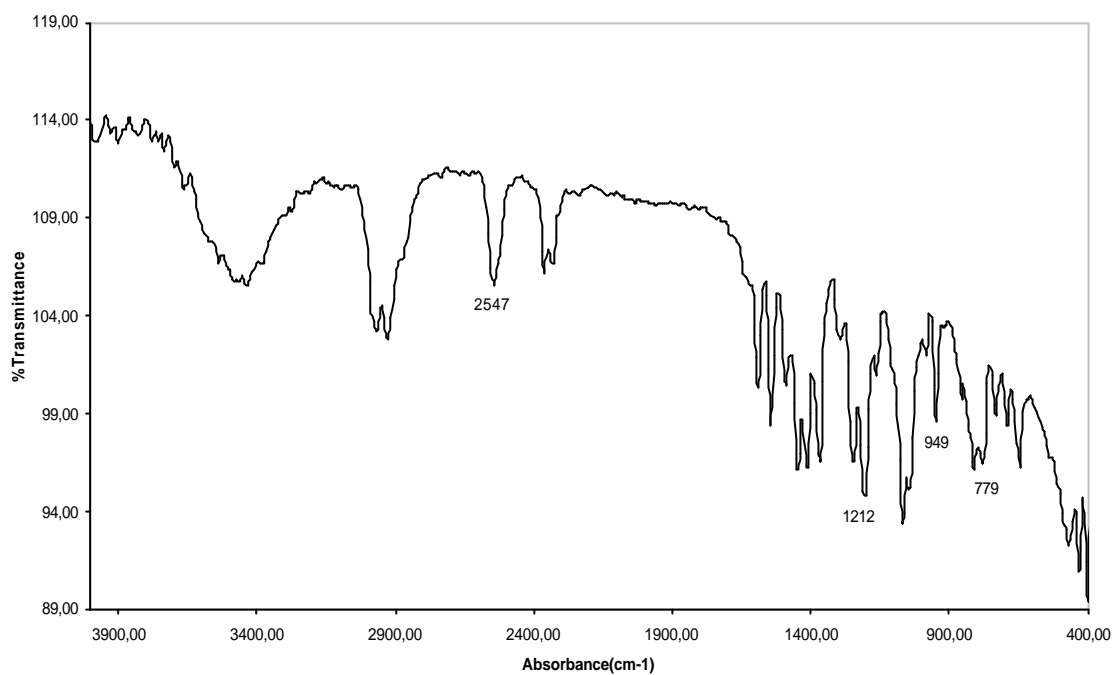


Figure 3.8. FT-IR spectrum of $[\text{MoTp}^*(\text{O})\text{Cl}](\mu\text{-O}) [\text{MoTp}^*\text{Cl}(\text{°NC}_6\text{H}_4\text{OEt})](2)$

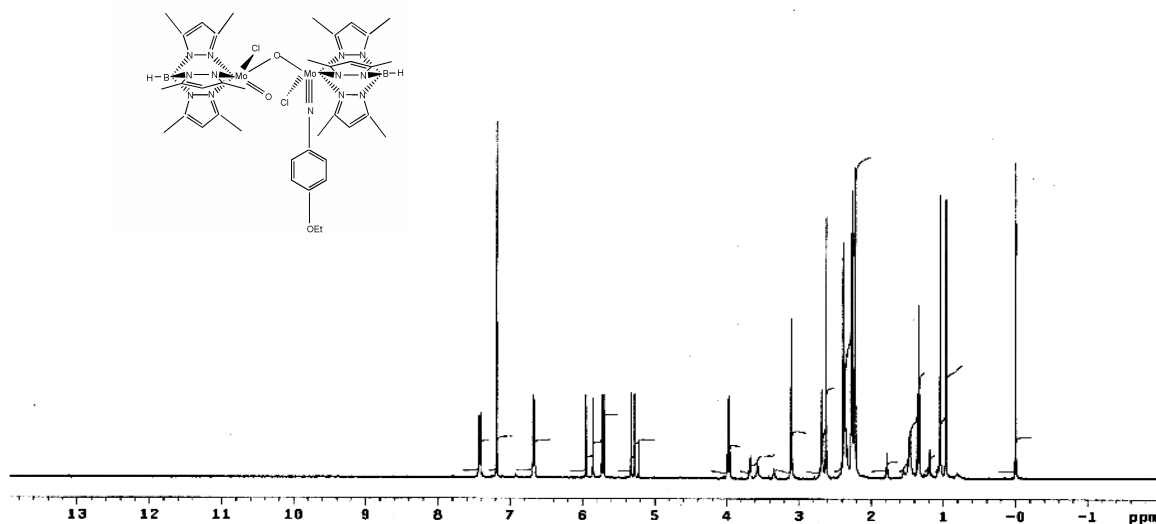


Figure 3.9. $^1\text{H-NMR}$ spectrum of $[\text{MoTp}^*(\text{O})\text{Cl}](\mu\text{-O}) [\text{MoTp}^*\text{Cl}(\text{°NC}_6\text{H}_4\text{OEt})](2)$

Table 3.6. ^1H -NMR data of $[\text{MoTp}^*(\text{O})\text{Cl}](\mu\text{-O}) [\text{MoTp}^*\text{Cl}(\text{O}^\circ\text{NC}_6\text{H}_4\text{OEt})]$ (2)

A^c	d^b / p.p.m	Assignment
2	7,48	d, $\text{NC}_6\text{H}_4\text{OEt}$ J(HH) 9
2	6,74	d, $\text{NC}_6\text{H}_4\text{OEt}$ J(HH) 9
1	6,02	s, $\text{Me}_2\text{C}_3\text{HN}_2$
1	5,92	s, $\text{Me}_2\text{C}_3\text{HN}_2$
1	5,79	s, $\text{Me}_2\text{C}_3\text{HN}_2$
1	5,77	s, $\text{Me}_2\text{C}_3\text{HN}_2$
1	5,39	s, $\text{Me}_2\text{C}_3\text{HN}_2$
1	5,34	s, $\text{Me}_2\text{C}_3\text{HN}_2$
2	4,04	q, OCH_2CH_3
3	1,41	t, OCH_2CH_3
36	2,29-3,17	s, $\text{Me}_2\text{C}_3\text{HN}_2$

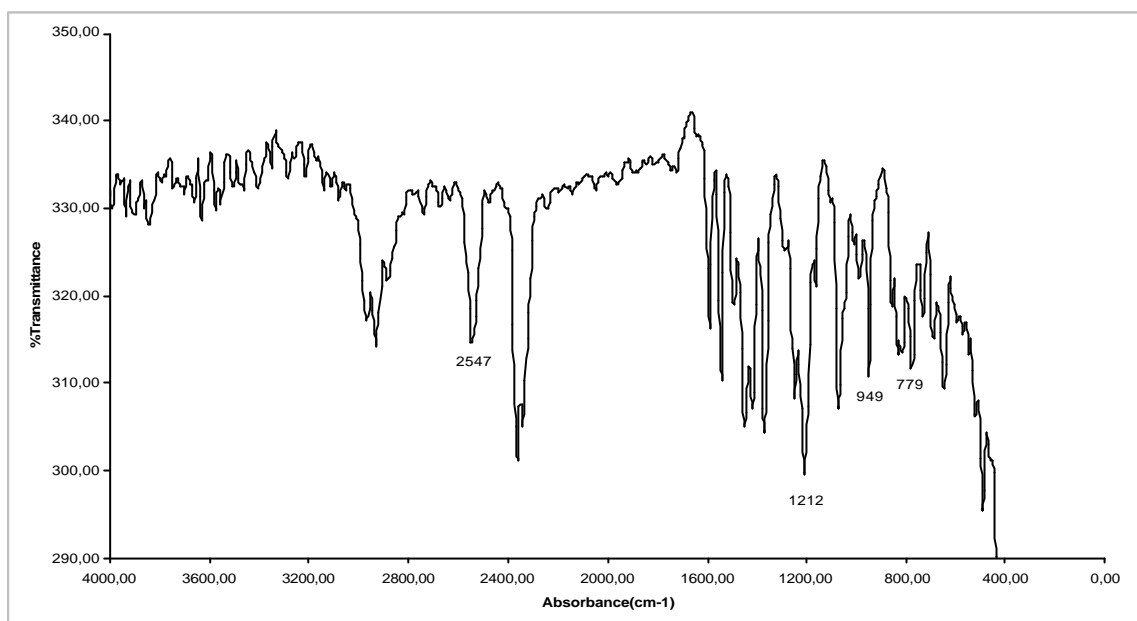


Figure3.10. FT-IR spectrum of $[\text{MoTp}^*(\text{O})\text{Cl}](\mu\text{-O}) [\text{MoTp}^*\text{Cl}(\text{°NC}_6\text{H}_4\text{OPr})]$ (3)

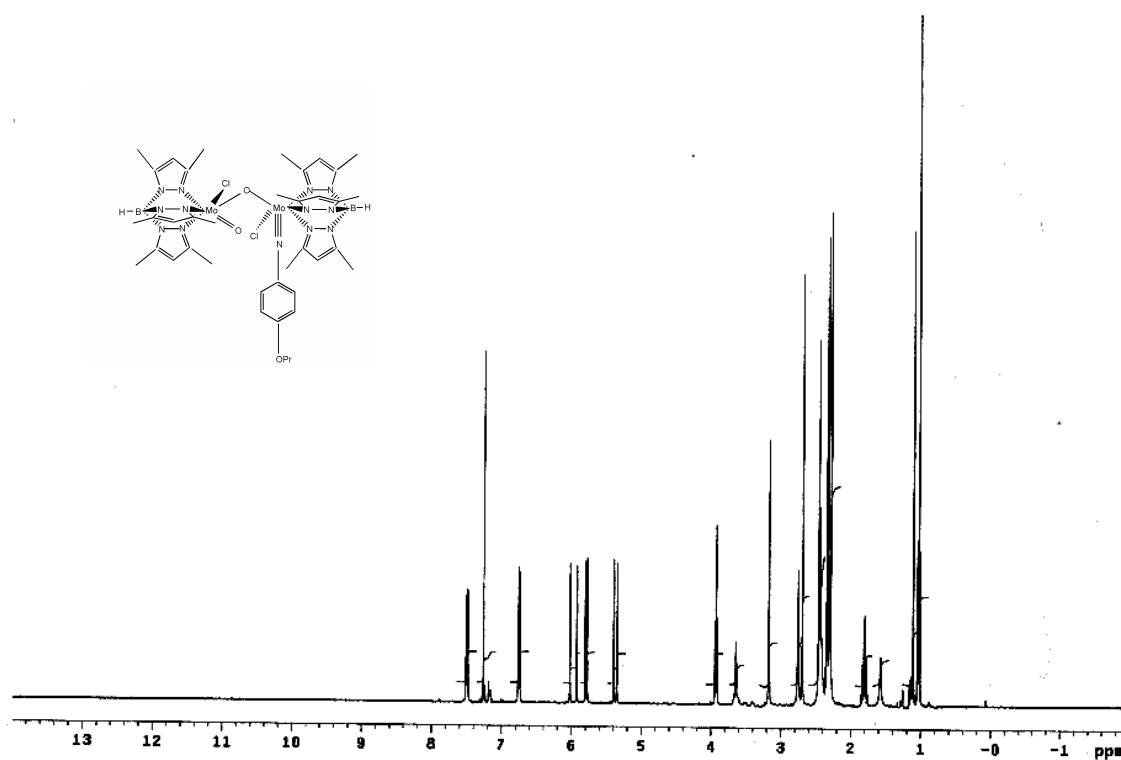


Figure3.11. $^1\text{H-NMR}$ spectrum of $[\text{MoTp}^*(\text{O})\text{Cl}](\mu\text{-O}) [\text{MoTp}^*\text{Cl}(\text{°NC}_6\text{H}_4\text{OPr})]$ (3)

Table 3.7. $^1\text{H-NMR}$ data of $[\text{MoTp}^*(\text{O})\text{Cl}](\mu\text{-O})[\text{MoTp}^*\text{Cl}(\text{O}^-\text{NC}_6\text{H}_4\text{OPr})]$ (3)

A^C	$d^b/p.p.m$	Assignment
2	7,49	d, $\text{NC}_6\text{H}_4\text{OPr}$ J(HH) 9
2	6,75	d, $\text{NC}_6\text{H}_4\text{OPr}$ J(HH) 9
1	6,02	s, $\text{Me}_2\text{C}_3\text{HN}_2$
1	5,92	s, $\text{Me}_2\text{C}_3\text{HN}_2$
1	5,8	s, $\text{Me}_2\text{C}_3\text{HN}_2$
1	5,79	s, $\text{Me}_2\text{C}_3\text{HN}_2$
1	5,4	s, $\text{Me}_2\text{C}_3\text{HN}_2$
1	5,35	s, $\text{Me}_2\text{C}_3\text{HN}_2$
2	3,93	t, $\text{OCH}_2\text{CH}_2\text{CH}_3$
3	1,8	m, $\text{OCH}_2\text{CH}_2\text{CH}_3$
3	1,03	t, $\text{OCH}_2\text{CH}_2\text{CH}_3$
36	2,29-3,17	s, $\text{Me}_2\text{C}_3\text{HN}_2$

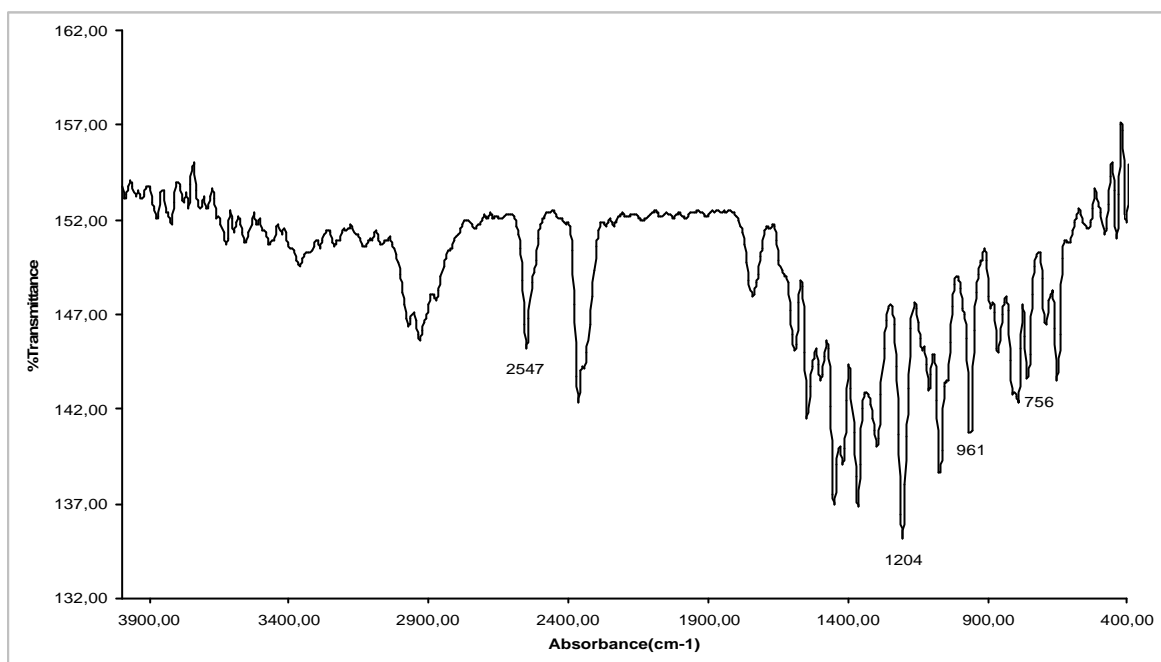


Figure 3.12. FT-IR spectrum of $[\text{MoTp}^*(\text{O})\text{Cl}](\mu\text{-O}) [\text{MoTp}^*\text{Cl}(\text{°NC}_6\text{H}_4\text{NO}_2)]$ (4)

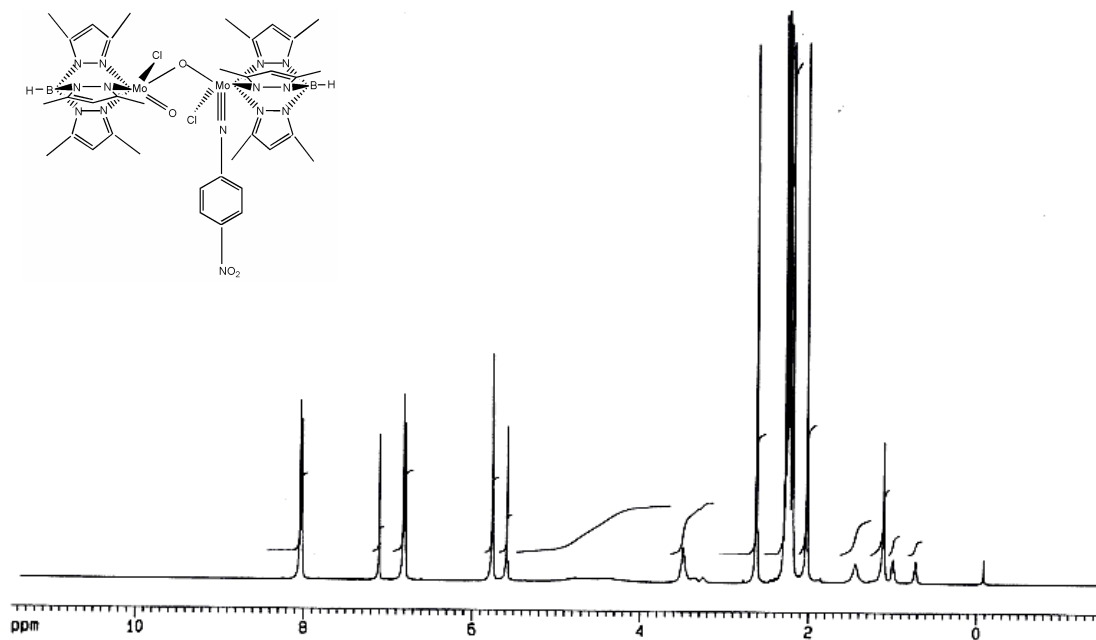


Figure 3.13. $^1\text{H-NMR}$ spectrum of $[\text{MoTp}^*(\text{O})\text{Cl}](\mu\text{-O}) [\text{MoTp}^*\text{Cl}(\text{°NC}_6\text{H}_4\text{NO}_2)]$ (4)

Table 3.8. $^1\text{H-NMR}$ data of $[\text{MoTp}^*(\text{O})\text{Cl}](\mu\text{-O}) [\text{MoTp}^*\text{Cl}(\text{}^o\text{NC}_6\text{H}_4\text{NO}_2)]$ (4)

A^c	d^b / p.p.m	Assignment
2	8,12	d, $\text{NC}_6\text{H}_4\text{NO}_2$ J(HH) 9
2	6,9	d, $\text{NC}_6\text{H}_4\text{NO}_2$ J(HH) 9
4	5,85	s, $\text{Me}_2\text{C}_3\text{HN}_2$
2	5,68	s, $\text{Me}_2\text{C}_3\text{HN}_2$
36	2,71-2,12	s, $\text{Me}_2\text{C}_3\text{HN}_2$

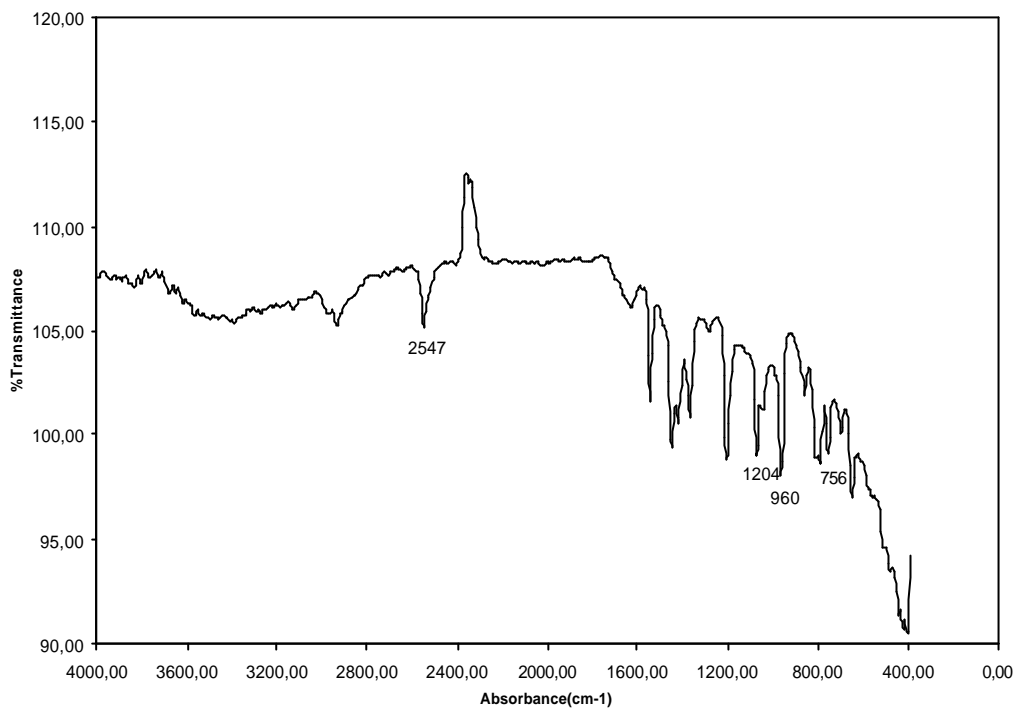


Figure 3.14. FT-IR spectrum of [MoTp*(O)Cl](μ-O) [MoTp*Cl(O)] (5)

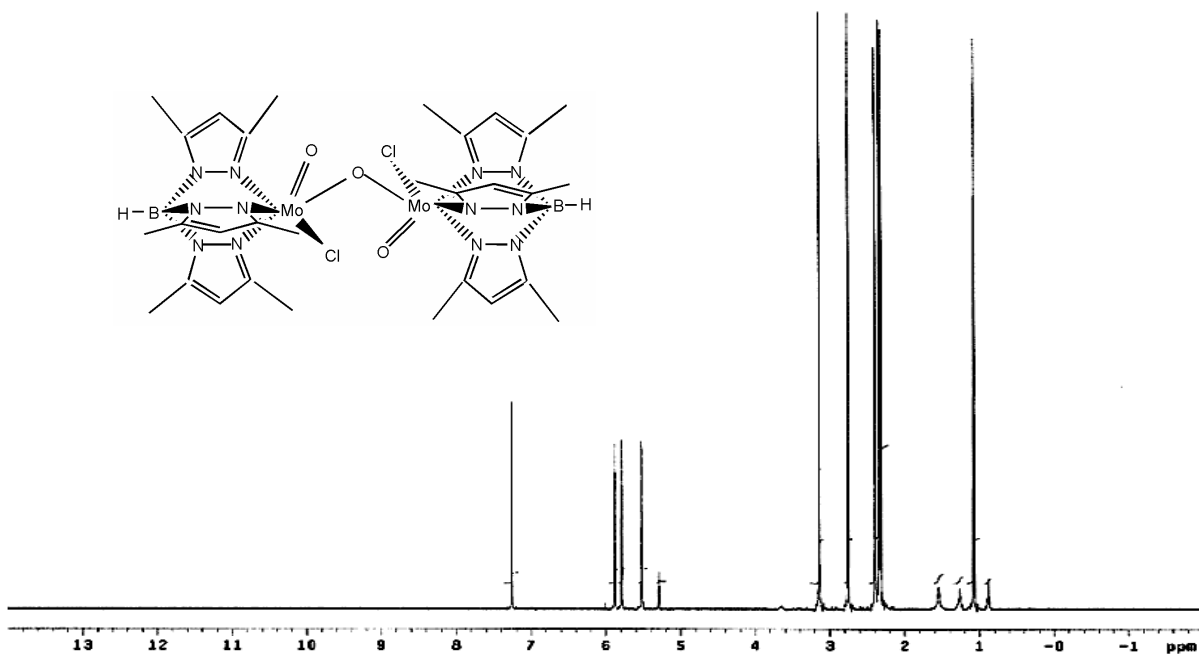


Figure 3.15. ¹H-NMR spectrum of [MoTp*(O)Cl](μ-O) [MoTp*Cl(O)] (5)

Table 3.9. $^1\text{H-NMR}$ data of $[\text{MoTp}^*(\text{O})\text{Cl}](\mu\text{-O})[\text{MoTp}^*\text{Cl}(\text{O})](5)$

A^c	$d^b/ \text{p.p.m}$	Assignment
2	5,88	s, $\text{Me}_2\text{C}_3\text{HN}_2$
2	5,79	s, $\text{Me}_2\text{C}_3\text{HN}_2$
2	5,52	s, $\text{Me}_2\text{C}_3\text{HN}_2$
36	2,32-3,14	$\text{Me}_2\text{C}_3\text{HN}_2$

Molecular ion peaks (Table 3.10) determined from the mass spectrometric data are in accord with the suggested structure for $[\text{MoTp}^*(\text{O})\text{Cl}](\mu\text{-O})[\text{MoTp}^*(\text{Cl})(\equiv\text{NC}_6\text{H}_4\text{X})]$ (X: OMe, OEt, OPr, NO_2) and the structure obtained by the X-ray structure of $[\text{MoTp}^*(\text{O})\text{Cl}](\mu\text{-O})[\text{MoTp}^*(\text{Cl})(\equiv\text{NC}_6\text{H}_4\text{OMe})]$ (Figure 3.4). No general trend for the rest of the fragmentation in the molecules could be determined.

Table 3.10. FAB-Mass data of the new complexes (1) and (4)

Compound	Mol wt.	M^+	$M^+ - \text{Cl}$
(1)	1012,4	1012,1	976,65
(4)	1025,3	1029,5	994,1

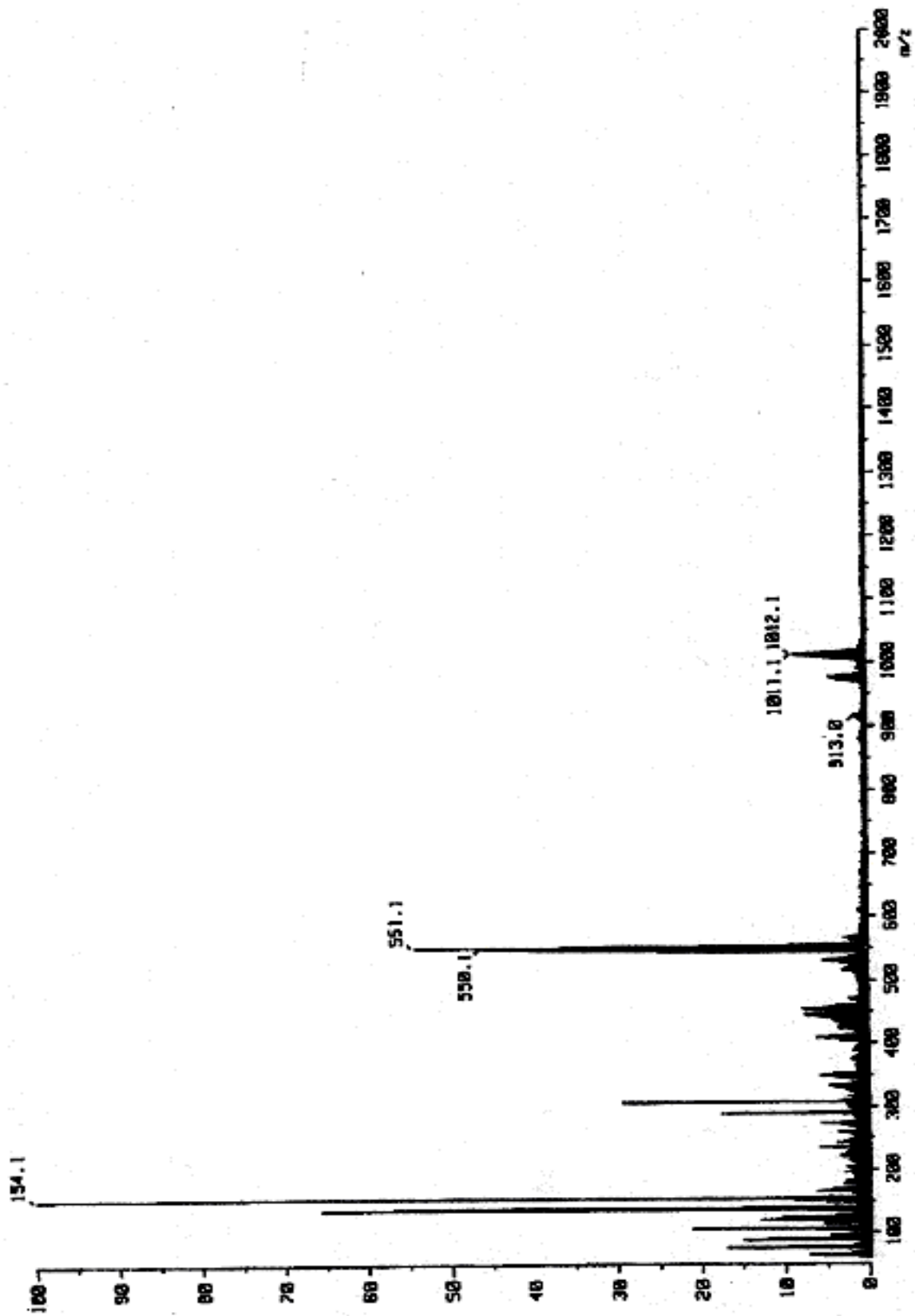


Figure 3.16. FAB-Mass spectrum of $[\text{MoTp}^*(\text{O})\text{Cl}](\mu\text{-O}) [\text{MoTp}^*\text{Cl}(\text{°NC}_6\text{H}_4\text{OMe})]$ (1)

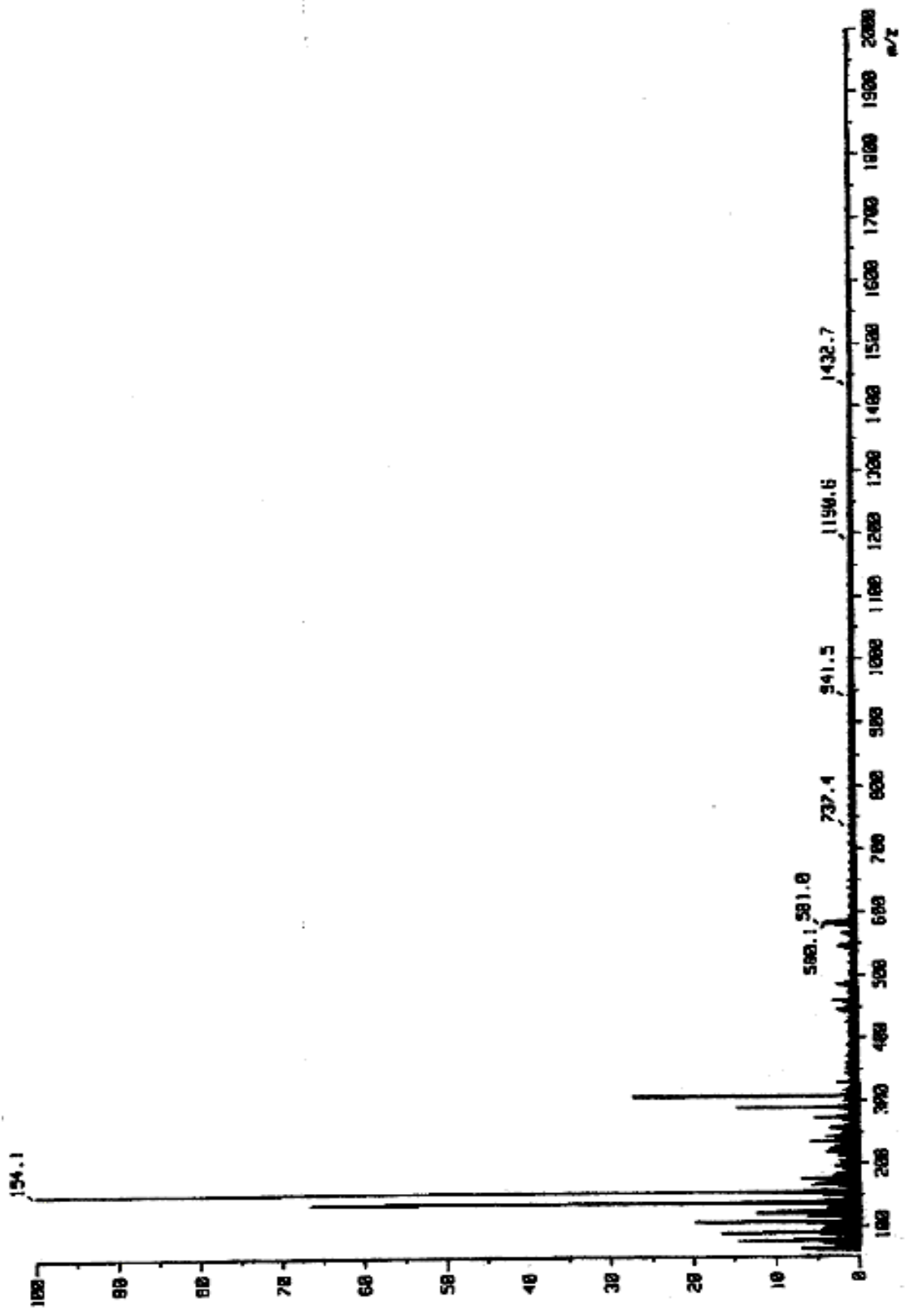


Figure 3.17. FAB-Mass spectrum of $[\text{MoTp}^*(\text{O})\text{Cl}](\mu\text{-O}) [\text{MoTp}^*\text{Cl}(\text{°NC}_6\text{H}_4\text{NO}_2)](4)$

CHAPTER 4

CONCLUSION

In this work, the reaction of the oxo Mo(V) precursor $[\text{MoTp}^*(\text{O})\text{Cl}_2]$ with *p*-substituted anilines were investigated. In all reactions regardless to the “R” substituent on the C_6H_4 ring, the novel oxo-bridged oxo(arylimido) Mo(V) compounds, $[\text{MoTp}^*(\text{O})\text{Cl}](\mu\text{-O}) [\text{MoTp}^*\text{Cl}(\equiv\text{NC}_6\text{H}_4\text{R})]$ (R = OMe, OEt, OPr, NO_2) were obtained by double deprotonation of the anilines.

The previously reported similar compounds were generally prepared in water or in aqueous media therefore, the synthetic method suggested for the new compound is interesting.

The new compounds are stable in air and soluble in polar organic solvents. They did not exhibit any fluxionality in solution.

The novel compounds described in this work is attractive in terms of molybdenum trispyrazolyl borate chemistry. Although a number of transition metal imido species containing hydrotris(pyrazolyl)borate type ligands and a number of systems involving μ -ligation in the presence of terminal imido groups have previously been reported, the chemistry of molybdenum compounds having arylimido and μ -oxo group in the presence of tris(3,5-dimethylpyrazolyl)borate co-ligand has not been explored widely.

REFERENCES

- [1] The term “bidentate” alone all too frequently implies “chelate” chelating bidentate ligand is called endobidentate and a bidentate ligand which cannot form a chelate but has to bond to two separate metals or metalloids an “exobidentate” ligand.
- [2] S.Trofimenko, “The Coordination Chemistry of Pyrazole-Derived Ligands,” *Chem. Rev.*, 72, (1972), 497-509
- [3] S.Trofimenko, “Boron-Pyrazole Chemistry” *J. Am. Chem. Soc.*, 88, (1966), 1842
- [4] J.P.Jesson, S.Trofimenko, and D.R.Eaton, “Spectra and structures of some transition metal poly(1-pyrazolyl)borates” *J. Am. Chem. Soc.*, 89, (1967), 3148
- [5] S.Trofimenko “Boron-pyrazole chemistry. II. Poly (1-pyrazolyl)-borates” *J. Am. Chem. Soc.*, 89, (1967), 3170
- [6] J.H.Enemark and K.B.Swedo, “Some aspects of the bioinorganic chemistry of molybdenum (RS)” *J. Chem. Edu.*, 56(2), (1979)
- [7] D.L.Reger, S.S.Mason and A.L.Rheingold, “Synthesis, structures, ¹¹³Cd solution NMR chemical shifts and investigations of fluxional processes of bis[poly(pyrazolyl)borato]cadmium complexes” *Inorg. Chem.*, 32, (1993), 5216
- [8] M.S.Sanford, L.M.Henling, R.H.Grubbs, “Synthesis and reactivity of neutral and cationic Ruthenium(II) tris(pyrazolyl)borate alkylidines” *Organometallics* 17, 5384, (1998)
- [9] S.Trofimenko, “Scorpionates-/the coordination chemistry of polypyrazolyl-borate ligands” *Imperial Collage Pres, London*, (1999)
- [10] M.D.Ward, J.A.McCleverty and J.C.Jeffery, “Coordination and supramolecular chemistry of multinucleating ligands containing two or more pyrazolyl-pyridine ‘arms’” *Coord. Chem. Rev.*, 222, 251, (2001)
- [11] S.Trofimenko, “Polypyrazolylborates, a new class of ligands” *Acc. Chem. Res.* 4, (1971), 17
- [12] S.Trofimenko, “Recent Advances in Poly(pyrazolyl) borate (Scorpionate) Chemistry” *Chem. Rev.*, 93, (1973), 943
- [13] S.Trofimenko, “Anomalous Reactions of Sterically Hindered Molybdenum Carbonyl Anions” *Inorg. Chem.*, 10, (1971), 504
- [14] S.Trofimenko, “Transition metal polypyrazolylborates containing other ligands” *J. Am. Chem. Soc.*, 91, (1969), 588

- [15] J.A.McCleverty and D.Seddon, "The chemistry of η^5 -Cyclopentadienyl Nitrosyl Molybdenum Complexes Part III. Dichloro and Dibromo Compounds and Their Lewis Base Adducts." *J.Chem.Soc. Dalton Trans.* 22, (1972), 2526
- [16] T.A.James and J.A.McCleverty "Transition-metal dithiolene complexes. Part XV. η^5 -Cyclopentadienyl nitrosyl and related molybdenum complexes" *J.Chem.Soc(A)*(1970) 3308-3314
- [17] N.Burzlauff , I. Hegelmann, B. Weibert "Bis(pyrazol-1-yl)acetates as tripodal "scorpionate" ligands in transition metal carbonyl chemistry: syntheses, structures and reactivity of manganese and rhenium carbonyl complexes of the type $[LM(CO)_3]$ (L=bpza, bdmpza)" *J. Organomet. Chem.* 626 (2001) 16–23 and references therein
- [18] C.D. Garner, C.M. Charnock, in: G. Wilkinson, R. D. Gilliard and J.A.McCleverty, (Eds.), *Comp. Coord. Chem.*, Pergamon Press, Oxford, 1987, p.1323.
- [19] D. Sellmann, B. Hadawi, F. Knoch and M. Moll, "Transition-Metal Complexes with Sulfur Ligands. 113. Syntheses, X-ray Crystal Structures, and Reactivity of Molybdenum(II) Complexes with Thioetherthiolate Ligands Having XS4 Donor Atom Sets (X = S, O, NH)" *Inorg. Chem.*, 34, 5963 (1995).
- [20] A.Galindo, F.Montilla, A.Pastor, E.Carmona, E.Puebla and C Ruiz " Synthesis and characterization (2,4,6-Trimethylphenylimido)molybdenum complexes. X-ray crystal structures of $(L_{OEt})Mo(Nmes)_2Cl$, $(L_{OEt})Mo(Nmes)Cl_2$, and $MoCl_3(Nmes)(depe)$ (mes = 2,4,6-Trimethylphenyl, L_{OEt} = (?-C₅H₅)Co{P(O)OEt₂}₃, depe = Et₂PCH₂CH₂PEt₂)" *Inorg. Chem.*, 36, 2379 (1997).
- [21] V.C.Gibson, C.Redshaw, G.L.P.Walker, W. Clegg, M.R.J. Elsegood "Synthesis, characterization and reactivity of the molybdenum(VI) complex $[MoCl(NAr)_2(CH_2CMe_2Ph)]$ (Ar=2,6-Prⁱ₂C₆H₃)" *J. Organomet. Chem.* 689 (2004) 332–344
- [22] H.Y.Cho, Soo-G. Roh, J.H.Jeong "Syntheses and reactivities of new bis(imido)Mo(VI) complexes of hydrotris(3,5-dimethyl-1-pyrazolyl)borate and X-ray molecular structures of $[{HB(3,5-Me_2C_3N_2H)_3}Mo(Nmes)_2X]$ (X : Cl or OH; mes : 2,4,6-trimethylphenyl)" *Polyhedron* 21 (2002) 1211- 1215

- [23] K. A. Rufanov, D.N.Zarubin, N.A.Ustynyuk, D.N.Gourevitch, J.Sundermeyer, A.V.Churakov, J.A.K.Howard, "Synthesis and structure of a series of new haloaryl imido complexes of molybdenum" *Polyhedron* 20 (2001) 379–385
- [24] H.H.Fox, K.B.Yap, J.Robbins, S.Cai, and R.R.Schrock "Simple, High-Yield Syntheses of Molybdenum(VI) Bis(imido) Complexes of the Type Mo(NR)₂C₁₂(1,2-dimethoxyethane)" *Inorg. Chem.*, (1992), 31, 2287-2289
- [25] M.C.W. Chan, F.W.Lee, K.K.Cheung and C.M.Che "Synthetic, structural and electrochemical studies of cationic chromium(VI) and molybdenum(VI) bis(imido) complexes supported by 1,4,7-triazacyclononane macrocycles", *J. Chem. Soc., Dalton Trans.*, (1999), 3197–3201
- [26] E.I. Stiefel, in : G. Wilkinson, R.D. Gillard and J.A. McCleverty, (Eds), *Comp.Coord. Chem.*, (1987), p. 1375.
- [27] S.Lee, R. Kowallick, M.Marcaccio, J.A.McCleverty and M.D.Ward "A new route to mixed oxo/arylimido complexes of molybdenum(VI) with a tris(pyrazolyl)borate co-ligand: synthesis, spectroscopic properties and ligand-centered redox activity" *J.Chem.Soc. Dalton Trans.*, 1998, 3443-3450 and references therein
- [28] G.R.Clark, A.J. Nielson and C.E.F. Rickard, "Preparation and crystal structure of an oxoimido complex of molybdenum containing the 2,4,6-triphenylphenylimide ligand" *J.Chem.Soc. Dalton Trans.*, (1996), 4265 – 4268
- [29] R.C.B. Copley, P.W.Dyer, V.C. Gibson, J.A.K. Howard, E.L.Marshall, W.Wang and B.Whittle, "Molybdenum(VI) complexes containing differing *cis* multiply-bonded ligands: Some structural consequences of competing p-donor groups" *Polyhedron*, (1996), 15, 3001
- [30] W.M. Vaughan, K.A.Abboud and J.M.Boncella, "Synthesis of a tris(pyrazolyl) borate-stabilized molybdenum alkylidene and its hydrolysis products. Crystal structures of TpMo(CH₂C(Me)₂Ph) (NAr)(O) and [TpMo(NAr)(O)]₂O" *J. Organomet.Chem.*, (1995), 485, 37-43
- [31] T.A. Coffey, G.D.Forster and G.Hogarth, "Synthesis and structural characterisation of dithiocarbamate-stabilised dimeric molybdenum(V) imido complexes via oxo substitution reactions with organic isocyanates" *J.Chem.Soc. Dalton Trans.*, (1995), 2337

- [32] V.C. Gibson, C.Redshaw, W. Clegg, M.R.J. Elsegood, U. Siemeling and T. Turk, "Synthesis and X-ray crystal structures of hydridotris(3,5-dimethylpyrazolyl)borate(Tp') molybdenum(IV) bis(imido) complexes" *Polyhedron*, (2004), 23, 189
- [33] M.Millar, S.Lincoln, S.A.Koch, "Stable monomeric complexes of molybdenum(III) and tungsten(III)" *J.Am.Chem.Soc.*, (1982), 104, 288
- [34] S. Lincoln, S.A. Koch "Synthesis, structure and interconversion of polypyrazolylborate complexes of molybdenum(V)" *Inorg. Chem.*, 1986, 25, 1594-1602
- [35] W.E.Cleland,Jr, K.M.Bernhart, K.Yamanouchi, D.Collison, F.E.Mabbs, R.B.Ortega and J.H.Enemark "Synthesis, structures and spectroscopic properties of six-coordinate mononuclear oxo-molybdenum(V) complexes stabilized by the hydrotris(3,5-dimethyl-1-pyrazolyl)borate ligand" *Inorg. Chem.*, (1987), 26, 1017-1025
- [36] V.An Ung, D.A.Bardwell, J.C.Jeffery, J.P.Maher, J.A.McCleverty, M.D.Ward, A.Williamson "Dinuclear oxomolybdenum(V) complexes showing strong interactions across diphenol bridging ligands: syntheses, structures, electrochemical properties and EPR spectroscopic properties" *Inorg. Chem.*, (1996), 35, 5290-5299
- [37] C.J. Chang, T.J. Pecci, M.D.Carducci, and J.H. Enemark "Synthesis and Characterization of Mononuclear Bis(para-substituted phenolato)oxomolybdenum(V) Complexes: Dependence of the Molecular Properties upon Remote Substituent Effects" *Inorg. Chem.*, (1993), 32, 4106-4110
- [38] P.Basu, M.A. Bruck, Z. Li, I.K. Dhawan, and J.H. Enemark "Molecular Structure and Electronic Properties of Oxomolybdenum(V) Catecholate Complexes" *Inorg. Chem.*, 1995, 34, 405-407
- [39] C.J. Chang and J.H. Enemark "Spectroscopic and Electrochemical Studies of Monomeric Oxomolybdenum(V) Complexes with Five-Membered Chelate Rings and Alkoxo or Alkanethiolato Ligands" *Inorg. Chem.* 1991, 30, 683-688
- [40] S.E. Lincoln, and T. M. Loehr "Chemistry and Electronic and Vibrational Spectroscopy of Mononuclear and Dinuclear (Tris(1-pyrazolyl)borato)- and Chloromolybdenum(V)-Oxo Complexes" *Inorg. Chem.*, (1990), 29, 1907-1915

- [41] Z. Xiao, J.H. Enemark, A.G. Wedd, and C.G. Young "Isovalent and Mixed-Valent Dinuclear μ -Oxo and μ -Oxo μ -Disulfido Complexes of Molybdenum(V) and Molybdenum(VI)" *Inorg. Chem.*, (1994), 33, 3438-3441
- [42] A.J.Millar, C.J.Doonan, L.J.Laughlin, E.R.T.Tiekink, C.G. Young "Atom transfer chemistry and electrochemical behavior of Mo(VI) and Mo(V) trispyrazolylborate complexes: new mononuclear and dinuclear species" *Inorg. Chim. Acta*, 337 (2002) 393-406
- [43] S. A. Roberts, C. G. Young, C.A. Kipke, W. E. Cleland, Jr., K. Yamanouchi, M. D. Carducci, and I H. Enemark "Dioxomolybdenum(VI) Complexes of the Hydrotris(3,5-dimethyl- 1-pyrazolyl) borate Ligand. Synthesis and Oxygen Atom Transfer Reactions" *Inorg. Chem.*, (1990), 29, 3650-3656
- [44] M.B.Kassim, R.L.Paul, J.C.Jeffery, J.A.McCleverty, M.D.Ward "Synthesis, redox and UV-Vis spectroelectrochemical properties of mono- and dinuclear tris(pyrazolyl)borato-oxomolybdenum(IV) complexes with pyridine ligands" *Inorg. Chim. Acta*, 327 (2002) 160-168
- [45] A. A. Eagle, M.F. Mackay, and C.G. Young "Synthesis and Characterization of the Mixed-Valence Complex $\text{LMO}^{\text{V}}\text{OCI}(\mu\text{-O})\text{MO}^{\text{VI}}\text{O}_2\text{L}$ (L = Hydrotris(3,5-dimethyl- 1-pyrazolyl)borate)" *Inorg. Chem.*, (1991), 30, 1425-1428
- [46] D.F. Shriver "The Manipulation of Air Sensitive Compounds" *McGraw-Hill, New York*, (1969)
- [47] J.Leonard, B.Lygo, G.Procter "Advanced Practical Organic Chemistry" *published by Blackie Academic & Professional, an imprint of Chapman & Hall* (1995)
- [48] C.J.Barton, "In Techniques of Inorganic Chemistry" *Vol. III. H.B. Jonassen and A.Weissberger, eds., Wiley-Interscience, New York*, (1963)
- [49] L.M.Harwood, C.J. Moody, "Experimental Organic Chemistry" *University of Oxford*
- [50] P.K.A.Shonfield, A.Behrendt, J.C.Jeffery, J.P.Maher, J.A.McCleverty, E.Psillakis, M.D.Ward and C.Western, "Very weak electron-electron Exchange interactions in paramagnetic dinuclear tris(pyrazolyl)boratomolybdenum centres with extended bridging ligands: estimation of the Exchange coupling constant J by simulation of second-order EPR spectra" *J.Chem.Soc. Dalton Trans.*, (1999), 4341-4347

- [50] P.K.A.Shonfield, A.Behrendt, J.C.Jeffery, J.P.Maher, J.A.McClevarty, E.Psillakis, M.D.Ward and C.Western, "Very weak electron-electron Exchange interactions in paramagnetic dinuclear tris(pyrazolyl)boratomolybdenum centres with extended bridging ligands: estimation of the Exchange coupling constant J by simulation of second-order EPR spectra" *J.Chem.Soc. Dalton Trans.*, (1999), 4341-4347
- [51] S.Bayly, J.A.McClevarty, M.D.Ward, D.Gatteschi, and F.Totti, "Metal-Metal interactions as a function of bridging ligand topology: An electrochemical, spectroelectrochemical, and magnetic study on dinuclear Oxo-Mo(V) complexes with various isomers of dihydroxynaphthalene as bridging ligand" *Inorg. Chem.*, (2000), 39, 1288-1293
- [52] W.L. Madison, SMART Diffractometer Control Software, Bruker Analytical X-ray Instruments Inc., (1998).
- [53] W. L. Madison, SAINT integration software, Siemens Analytical X-ray Instruments Inc., (1994)
- [54] G.M. Sheldrick, SADABS: A program for absorption correction with the Siemens SMART system; (1996)
- [55] W.L. Madison, SHELXTL program system version 5.1; Bruker Analytical X-ray Instruments Inc., (1998)
- [56] International Tables for Crystallography, Kluwer, Dordrecht, (1992), C.
- [57] S. Lincoln and T.M. Loehr, *Abstracts of Papers of the Am.Chem. Soc.*, 200: 56-Inorganic Part 1 (1 990).
- [58] K.Dehnicke and J.Strahle, "The transition metal-nitrogen multiple bond" *Angew.Chem.*, 20, (1981), 413-486
- [59] J.A.McClevarty, G.Denti, S.J.Reynolds, A.S.Drane, N.El.Murr, A.E.Rae, N.A.Bailey, H.Adams, J.M.A.Smith, " Arylamido and aryloxy complexes of nitrosyl{tris(3,5-dimethylpyrazolyl)borato}molybdenum, some mixed alkoxy/aryloxy and aryloxy/monoalkylamido species, and the structures of $[\text{Mo}\{\text{HB}(3,5\text{-Me}_2\text{C}_3\text{HN}_2)_3\}(\text{NO})\text{I}(\text{NHC}_6\text{H}_4\text{R-P})]$, (R = Me and OMe)" *J.Chem.Soc. Dalton Trans.*, (1983), 81-9
- [60] J.A.McClevarty, B.D.Neaves, S.J.Reynolds, H.Adams, N.A.Bailey and G.Denti "Molybdenum and tungsten nitrosyl complexes containing alkoxy, aryloxy and

- arylamido ligands: their electrochemical behaviour and the structure of
[Mo{HB(Me₂pyz)₃}(NO)I{OCH₂)}₃Br}]” *J.Chem.Soc. Dalton Trans.*,1986, 733-41
- [61] D.E.Wigley, “Organoimido complex of the transition metals” *Prog., Inorg., Chem.*,(1994), 42, 239-482